https://doi.org/10.5194/egusphere-2024-800
Preprint. Discussion started: 2 April 2024

An improved Trajectory-mapped Ozonesonde dataset for the Stratosphere and Troposphere (TOST): update, validation and applications

Zhou Zang[1], Jane Liu[1], David Tarasick[2], Omid Moeini[2], Jianchun Bian[3], Jinqiang Zhang[3], Anne M. Thompson[4,5], Roeland Van Malderen[6], Herman G.J. Smit[7], Ryan M. Stauffer[4], Bryan J. Johnson[8] and Debra E. Kollonige[4,9]

[1]Department of Geography and Planning, University of Toronto, Toronto, Canada
[2]Environment and Climate Change Canada, Toronto, Canada
[3]Key Laboratory of Middle Atmosphere and Global Environment Observation, Institute of Atmospheric Physics, Chinese Academy of Sciences, Beijing, China
[4]Atmospheric Chemistry and Dynamics Laboratory, NASA Goddard Space Flight Center, Greenbelt, Maryland, USA
[5]University of Maryland Baltimore County, Baltimore, MD, USA
[6]Royal Meteorological Institute of Belgium, Brussels, Belgium
[7]Institute for Energy and Climate Research: Troposphere (IEK-8), Research Centre Juelich (FZJ), Juelich, Germany.
[8]NOAA/ESRL Global Monitoring Division, Boulder, Colorado, USA
[9]Science Systems and Applications, Inc., Lanham, MD, USA

Correspondence: Jane Liu (janejj.liu@utoronto.ca)

Abstract

A global-scale horizontally- and vertically-resolved ozone climatology can provide a detailed assessment of ozone variability. Here, the Trajectory-mapped Ozonesonde dataset for the Stratosphere and Troposphere (TOST) ozone climatology is improved and updated to the recent decade (1970s-2010s) on a grid of 5° × 5° × 1 km (latitude, longitude, and altitude) from the surface to 26 km altitude, with the most recent ozonesonde data re-evaluated following the ASOPOS-2 guidelines (GAW Report No. 268, 2021). Comparison between independent ozonesonde and trajectory-derived ozone shows good agreement in each decade, altitude, and station, with relative

https://doi.org/10.5194/egusphere-2024-800
Preprint. Discussion started: 2 April 2024

differences (RD) of 2-4% in the troposphere and 0.5% in the stratosphere. Comparisons of TOST with aircraft and two satellite datasets, the Satellite Aerosol and Gas Experiment (SAGE) and the Microwave Limb Sounder (MLS), show comparable overall agreement. The updated TOST outperforms the previous version with higher data coverage in all latitude bands and altitudes and 14-17% lower RD compared to independent ozonesondes, employing twice as many ozonesonde profiles and an updated trajectory simulation model. Higher uncertainties in TOST are where data are sparse, i.e., over the southern high latitudes and the tropics, and before the 1980s, and where variability is high, i.e., at the surface and upper troposphere and lower stratosphere (UTLS). Caution should therefore be taken when using TOST in these spaces and times. TOST captures global ozone distributions and temporal variations, showing an overall insignificant change of stratospheric ozone after 1998. TOST offers users a long record, global coverage, and high vertical resolution.

1. Introduction

The global ozone distribution and its long-term changes at different altitudes, longitudes, and latitudes are critical to understanding global ozone variability and its interactions with climate change. While the ozone trends themselves can indicate the impact of changes in climatic dynamics (Hassler et al., 2008), or chemistry, including the effect of the Montreal Protocol (Steinbrecht et al., 2017), long-term horizontally- and vertically-resolved ozone are needed for prescribing, evaluating and refining ozone simulations in climate models (Hassler et al., 2018), and to quantify changes in radiative forcing and projecting reliable future climate scenarios (Nowack et al., 2015).

Balloon-borne ozonesondes are the principal source of trend-quality long-term records of ozone profiles below ~18 km (Tarasick et al., 2021). However, the horizontal and temporal

https://doi.org/10.5194/egusphere-2024-800
Preprint. Discussion started: 2 April 2024

coverages of ozonesondes are limited by the sparse distribution of the stations (less than 100 worldwide) and their low launch frequency (1-3 times/week) (Liu et al., 2013a). The In-Service Aircraft for a Global Observing System (IAGOS) program has measured ozone profiles worldwide since 1994 via the instruments onboard a number of commercial aircraft, with high sampling frequency at some airports (Thouret et al., 1998). However, sampling is unevenly distributed both spatially and temporally because the flights are constrained by commercial airlines' operation schedules. Satellite observations have the advantage of providing large-scale 3-dimensional ozone data with consistent quality. However, satellite data are provided for the stratosphere only or for troposphere with limited vertical resolution (6–10 km) (Worden et al., 2007; Liu et al., 2010; Tarasick et al., 2019b) caused by uncertainties for satellites to retrieve tropospheric ozone through the large stratospheric ozone burden (Bhartia, 2002). A number of studies have developed long-term (since the 1980s) ozone climatologies by combining ozone data from ozonesondes and/or multiple satellite instruments (McPeters et al., 2007; McPeters and Labow, 2012; Hassler et al., 2018; Bodeker et al., 2021; Bognar et al., 2022), but these are generally zonally-averaged. Chemistry–climate models are also used to develop 3-dimensional ozone data fields, especially for long-term, global-scale simulations (Eyring et al., 2010; Chen et al., 2018); these models present our best understanding of processes controlling ozone variationsbut still suffer from large uncertainties regarding the inventories, parameterizations, radiation transport schemes, and simulation of the atmospheric circulations and systems (Young et al., 2018; Wild et al., 2020; Griffiths et al., 2021; Zeng et al., 2022).

Liu et al. (2013a, b) constructed a long-term 3-dimensional global-scale ozone dataset using a trajectory-mapping method, extending sparse ozonesonde measurements and filling gaps in the spatial domain by backward and forward trajectory simulations. The trajectory-mapping method assumes the ozone mixing ratio in the same air parcel along each trajectory path is constant for

https://doi.org/10.5194/egusphere-2024-800
Preprint. Discussion started: 2 April 2024

several days, which is reasonable given that the lifetime of ozone in most of the troposphere and stratosphere ranges from weeks to months (Jacob, 1999). The result is a global dataset that is independent of satellite measurements and photochemical modeling processes. The trajectory-mapping method can be characterized as a meteorologically-guided interpolation method, which necessarily carries more information than conventional statistical interpolation methods (Stohl et al., 2001). In addition, the trajectory-derived ozone data cover higher latitudes (to 90ºN and 90ºS) and a longer time period (since the 1960s) (Liu et al., 2013b). The Trajectory-mapped Ozonesonde dataset for the Stratosphere and Troposphere (TOST) Version 1 is available from 1965-2012 at the World Ozone and UV Data Centre (WOUDC, https://woudc.org/archive/products/ozone/vertical-ozone-profile/ozonesonde/1.0/tost/, last access: Jan 29, 2024), and has been successfully applied in model evaluation (Skeie et al., 2020; Badia et al., 2021), ozone and climate trend studies (Polvani et al., 2017; Gaudel et al., 2018; Gulev et al., 2021), as a background ozone climatology (Xu et al., 2018; Moeini et al., 2020, and for tropospheric ozone burden estimation (Griffiths et al., 2021).

There have been several important developments since the publication of the first version of TOST data in 2013 (Liu et al. 2013a, b), which we refer to as TOST Version 1, or TOST-v1. An improved version of TOST, namely TOST-v2, is necessary for the following reasons. Firstly, there are some 50,000 new ozone profiles, many from newly established ozonesonde stations (see Section 2.1). These new ozonesonde data permit updating TOST to 2021, providing 3-dimensional ozone information through the 2010s. Secondly, data from many ozonesonde stations have been updated to higher-quality versions. An important source of uncertainty in TOST-v1 is possible biases in station records due to instrument changes and/or changes in operating procedures. Homogenized time series are now available from the Harmonization and Evaluation of Ground Based Instruments for Free Tropospheric Ozone Measurements (HEGIFTOM) project for over 40

https://doi.org/10.5194/egusphere-2024-800
Preprint. Discussion started: 2 April 2024

ozonesonde stations (Table S1). For these records, biases due to instrument changes, sensing solution, and preparation changes have been corrected, to reduce the overall uncertainty from 10-20% to 5-10% (Smit and Thompson, 2021). This effort to improve data quality also uncovered an apparent change of bias at stations flying one type of sonde (Stauffer et al., 2020; 2022); 14 global ozonesonde stations (the bolded stations in Table S1) have shown an apparent drop-off of 2-4 % in stratospheric ozone and total ozone column since circa 2013, due to a possible instrument artifact. This is the subject of ongoing research (e.g. https://gml.noaa.gov/annualconference/abstracts/78-230424-A.pdf, last access: Jan 29, 2024). For these stations, ozone measurements above 40 hPa (~20 km) are not recommended for trend calculations. We need therefore to exclude data above 40 hPa for the affected profiles in constructing TOST. Thirdly, the version 4.9 of the Hybrid Single-Particle Lagrangian Integrated Trajectory (HYSPLIT) model (Draxler and Hess, 1998) used for trajectory simulation has been improved and updated to version 5.2. Here, we address the mentioned issues and construct an improved and updated TOST using the most state-of-the-art HYSPLIT and most updated ozonesonde data. While Liu et al. (2013a, b) validated TOST-v1 with ozonesonde data at 20 selected stations, TOST-v2 is validated against the ozonesonde data at all 141 stations individually with the trajectory-mapped approach omitting the input from the station being tested. In addition, comparisons are made with the IAGOS measurements in the troposphere, and with two limb-viewing satellite sensors, the Satellite Aerosol and Gas Experiment (SAGE) and the Microwave Limb Sounder (MLS), in the stratosphere. This more comprehensive validation and associated uncertainty analysis demonstrates the improved quality of TOST-v2, and also provides some caveats for users of TOST.

In the following, Section 2 explains the data sources and the improved trajectory-mapping methodology. Section 3 presents independent validations, comparisons with satellite data, and improvements compared to TOST-v1, as well as the uncertainties in TOST-v2. Based on TOST-

https://doi.org/10.5194/egusphere-2024-800
Preprint. Discussion started: 2 April 2024

v2, we characterize global ozone variations in the troposphere and stratosphere, and show stagnant stratospheric ozone variation since the late 1990s in Section 4, followed by conclusions in Section 5.

2. Data and Methods

2.1 Ozonesonde data

Ozonesonde data over 1970-2021 at 141 ozonesonde stations worldwide (Figure 1) were downloaded from the World Ozone and Ultraviolet Radiation Data Centre (WOUDC, https://woudc.org/archive/Archive-NewFormat/OzoneSonde_1.0_1/), or where available, homogenized data from Southern Hemisphere ADditional OZonesondes (SHADOZ, https://doi.org/10.57721/SHADOZ-V06, last access: Jan 29, 2024) and HEGIFTOM (https://hegiftom.meteo.be/datasets/ozonesondes, last access: Jan 29, 2024). The homogenized ozonesonde stations from HEGIFTOM include ozonesonde stations from the SHADOZ network (Thompson et al., 2017; Witte et al., 2017; 2018), the Canadian network (Tarasick et al., 2016), the US network (Sterling et al., 2018), the Network for the Detection of Atmospheric Composition Change (NDACC) and several individual stations (Van Malderen et al., 2016; Witte et al., 2019; Ancellet et al., 2022), with an overall accuracy of 3-5% in both the stratosphere and troposphere. Ozonesonde data from the Beijing Nanjiao Meteorological Observatory (116.47°E, 39.81°N) in Beijing, China, are provided by the Institute of Atmospheric Physics (IAP), Chinese Academy of Sciences. The ozone profiles at Beijing are measured by the Brewer-Mast type GPSO3 ozonesonde and the IAP electrochemical concentration cell (ECC) ozonesonde, which are in fair agreement with commercial ECC ozonesondes (Wang et al., 2003; Xuan et al., 2004; Bian et al., 2007) in both laboratory and field experiments (Zhang et al., 2021; Zeng et al., 2023). In total, data from 43 more stations were used in this version of TOST than in TOST-v1 (Liu et al., 2013b).

https://doi.org/10.5194/egusphere-2024-800
Preprint. Discussion started: 2 April 2024

Figure 1a provides an overview of the distribution of the ozonesonde stations, the number of profiles, and the beginning year for every station. Most of the stations with data before the 1980s are located in North America, Europe, and East Asia. The majority of the stations in the Southern Hemisphere start measurement in the 1990s or later, and so the Southern Hemisphere contains a smaller number of ozone profiles than in the Northern Hemisphere. Figure 1b shows that the total number of ozonesonde profiles per year has almost doubled since the 1990s and reached a maximum in the late 2000s with over 3000 profiles per year. Since then, the available amount of ozonesonde profiles has declined slightly to 2000-3000 profiles per year. The average annual number of profiles per station slightly increased since the 1990s and has stabilized at about 40 profiles per year.

All the ozonesonde profiles were processed into 1-km vertical resolution by integrating and averaging the ozone volume mixing ratio in 1-km layers from the ground level. The ozonesonde data above 26 km were excluded as the data above this height show large uncertainties at mid- and high-latitudes (Fioletov et al., 2006).

2.2 Trajectory simulation

Forward and backward trajectories in four days were calculated every 6 hours using the version 5.2 HYSPLIT model (Stein et al., 2015). HYSPLIT was driven by the reanalysis of hourly meteorological data from the National Centers for Environmental Prediction/National Center for Atmospheric Research (NCEP/NCAR), which has a horizontal resolution of 2.5° by 2.5° in latitude and longitude and 17 vertical levels from the surface to 10 hPa (Kalney et al., 1996). The length of the trajectories influences the spatial coverage and accuracy of the ozone mapping. Generally, uncertainties increase rapidly along the trajectories, with typical errors of about 100–200 km day^{-1} (Stohl, 1998). Trajectories have horizontal uncertainties of 350–400 km after 3 days and 600-1000

https://doi.org/10.5194/egusphere-2024-800
Preprint. Discussion started: 2 April 2024

km after 4 days in the Northern Hemisphere (Engström and Magnusson, 2009). Trajectories show typical vertical deviations of about 200, 800, and 1000 m after 2, 4, and 6 days in the stratosphere, and even greater uncertainties in the troposphere (Stohl and Seibert, 1998). Therefore, to limit trajectory errors, 4-day trajectories were used herein, following previous studies (Tarasick et al., 2010; Liu et al., 2013 a, b).

2.3 Three-dimensional ozone mapping based on ozonesonde profiles and trajectories

Ozone mixing ratios from each sounding at the 26 levels were assigned to the corresponding forward and backward trajectory paths. These ozone values at positions every 6 hours along the 4-day backward and forward trajectories (32 positions for each level) were averaged in bins of 5° latitude and 5° longitude, for each 1-km altitude for every month. This bin size corresponds both to the typical uncertainties of 4-day trajectories discussed above, and to the typical ozone correlation length (500-1500 km) in the troposphere and the stratosphere (Liu et al., 2009). Ozonesonde profile data and trajectories in both the troposphere and stratosphere were used to represent the exchanges of ozone between the troposphere and stratosphere in ozone climatology. Based on this mapping, TOST was generated at 26 altitude levels in monthly means for each decade from the 1970s to the 2010s and in annual means for each year from 1970 to 2021.

Errors in the mapped data can come from trajectory errors, and from ignoring ozone chemistry (production and loss) along the transport pathway and deposition in the surface layer (Liu et al., 2013a). Differences between the results of backward and forward trajectory mapping can provide a measure of these errors, since in the absence of such errors the results of forward-only and backward-only trajectory mapping should be identical. Therefore, mappings from the forward-only and backward-only trajectories were compared as an initial quality check. Figure S1 shows monthly means (January and July) in 2000 at 3-4 km and 19-20 km, for forward-only and

https://doi.org/10.5194/egusphere-2024-800
Preprint. Discussion started: 2 April 2024

backward-only mapping. In general, the differences between the two mappings are commonly less than 15% and have no distinct pattern, indicating that trajectory errors, and those from ozone chemistry and deposition, are not systematic. These modest differences between forward-only and backward-only trajectory-mapped ozone fields also validate the reliability of this trajectory-mapping method; both backward and forward trajectories, therefore, were combined in TOST to achieve better averages and higher spatial coverage.

The resulting ozone fields are given in two altitude coordinates (altitude above sea level and altitude above ground level) for users' convenience. In addition, three ozone climatology datasets are generated based on trajectories from ozonesonde observations in both the troposphere and stratosphere, trajectories from observations only in the troposphere (troposphere-only) and trajectories from observations only in the stratosphere (stratosphere-only). Examples presented in this paper all use ozone mapping based on trajectories from observations in both the troposphere and stratosphere, with altitudes above sea level. For this coordinate system, both ozonesonde profiles and mapped data necessarily begin at the altitude of the surface, leaving the levels below as null.

2.4 Validations of TOST

To comprehensively validate TOST, several validations and comparisons were conducted.

2.4.1 Ozonesonde profiles for validation

The first method is to compare the actual ozone profile at each of the ozonesonde stations with the trajectory-derived ozone profile for that station without the input of that station itself. This method is computationally intensive, as the trajectory mapping must be re-calculated (with data for all stations except one), for each ozonesonde station, but it directly tests the reliability of deriving ozone concentrations at a location by integrating the contributions via trajectories from

https://doi.org/10.5194/egusphere-2024-800
Preprint. Discussion started: 2 April 2024

surrounding sites, which is the essential assumption of the trajectory-mapping method. We refer to this set of data that selectively excludes the local data at each station as "Traj-derived".

2.4.2 Satellite ozone profile data

TOST is further compared with two well-known satellite limb sounder datasets, the Satellite Aerosol and Gas Experiment (SAGE) and the Microwave Limb Sounder (MLS).

SAGE II was launched into a 57-degree inclination orbit on board Earth Radiation Budget Satellite (ERBS), and was in operation from 1984–2005. Using the highly accurate solar occultation technique, SAGE can resolve layers in the middle and upper troposphere at 1-km vertical resolution (Kent et al., 1993), with the highest accuracy over the 20-45 altitude range (Cunnold et al., 1996). Here we use the Version 7.0 SAGE II ozone mixing ratio (https://sage.nasa.gov/missions/about-sage-ii/, last access: Jan 29, 2024) in the 1980s and 1990s for the comparison.

The MLS, onboard the Aura satellite, can measure stratospheric ozone profiles with a vertical resolution of about 3 km. MLS observes microwave radiances that are both emitted and absorbed by the atmosphere. The retrieval is more complex, and uses the optimal estimation approach. Here we use the Version 5.0 MLS ozone mixing ratio (https://disc.gsfc.nasa.gov/datasets/ML2O3_005/summary?keywords=ML2O3_005, last access: Jan 29, 2024) in the 2000s and 2010s for the comparison.

2.4.3 Aircraft ozone profile data

The IAGOS network (https://www.iagos.org/, last access: Jan 29, 2024) has been measuring ozone profiles worldwide since 1994 via dual-beam ultraviolet absorption monitors onboard commercial aircraft (Petzold et al., 2015), with an accuracy of about ± (2 nmol mol^{-1} + 2%) (Nédélec et al., 2016). Ozone monitors are calibrated annually to a reference analyser at the Bureau Internationale des Poids et Mesures (BIPM), and also compared every 2 hours to an in-flight ozone calibration

https://doi.org/10.5194/egusphere-2024-800
Preprint. Discussion started: 2 April 2024

source. Generally good agreement is found between IAGOS profiles and ozonesondes, with positive biases for the sondes of 5-10% (Tilmes et al., 2012; Zbinden et al., 2013; Staufer et al., 2013, 2014; Tanimoto et al., 2015; Tarasick et al., 2019b), making IAGOS ozone suitable for the validation of TOST. Here, the IAGOS ozone profiles were processed into 1 km layers from sea level and matched with the TOST ozone for each level to examine the performance of TOST in the troposphere.

3. Validations and comparisons of TOST

3.1 Validations with ozonesonde observations

First, we show the overall comparison in monthly mean ozone profile between ozonesonde and trajectory-derived values without the inputs of the stations being tested (Traj-Derived), from all the existing stations at selected altitude levels. Note that the full TOST dataset would be better than "Traj-Derived ozone", especially at the sampling locations because the input of the local station is included in the full TOST data. The three altitude levels are selected to present the overall accuracy of TOST in the lower troposphere (ozone concentration at 0-50 ppbv,), the upper troposphere (ozone concentration at 50-150 ppbv) and the stratosphere (ozone concentration at >150 ppbv).

Figure 2a-e shows the overall tropospheric ozone comparisons between independent ozonesonde (Sonde-Observed) and Traj-Derived ozone in the entire study period (Figure 2a-c) and each decade (Figures 2d). Overall, the Sonde-Observed and Traj-Derived ozone concentrations agree well in the lower troposphere (Figure 2a), with a correlation coefficient (R) of 0.69 and a root mean square (RMS) difference [square root of the mean of squared individual differences] of 7.5 ppbv, a low bias (0.7 ppbv) and RD (1.8%) [where RD is the relative difference 100 × (TOST ozone - ozonesonde ozone)/ozonesonde ozone)]. The linear fit for the entire study period shows a

https://doi.org/10.5194/egusphere-2024-800
Preprint. Discussion started: 2 April 2024

slope of 0.99. In the upper troposphere (Figure 2b), the agreement between the Sonde-Observed and Traj-Derived ozone concentration is moderately lower, with a linear fitting coefficient of 1.01 and RMS of 21.1 ppbv, and higher bias (2.9 ppbv) and RD (4.0%) than those in the lower troposphere. This lower agreement in the upper troposphere owes to greater influence of stratosphere-to-troposphere (STE) in the upper troposphere, where trajectories by the Lagrangian dispersion model (such as HYSPLIT) show substantially increased deviations due to the strong turbulence and convection (Stohl et al., 2002). The positive bias may imply that STE is slightly overestimated in HYSPLIT, as the comparison between the Sonde-Observed and troposphere-only Traj-Derived ozone concentrations shows a clear underestimation (with RD of -9% to -5%) in the upper troposphere (Figure S2). In the stratosphere (Figure 2c), the overall agreement between the Sonde-Observed and Traj-Derived ozone concentrations has a linear fitting coefficient of 0.97 and an RMS of 416.9 ppbv. The small bias is of higher magnitude (11.1 ppbv) to that in the troposphere but this is much smaller relative to stratospheric ozone concentrations; the RD is only 0.5%, indicating higher reliability of Traj-Derived in the stratosphere.

This validation method compares ozonesonde station data with Traj-Derived ozone, i.e., the ozone found by averaging trajectories that come from other stations, some of which will have higher ozone, and some lower. The average difference results from an imbalance in the distribution of meteorological trajectories, and this is confirmed by detailed analysis. For example, before the 1990s, fitting coefficients were smaller than 1 and Rs were smaller than 0.60 (Figure 2d) in the lower troposphere, indicating a tendency to underestimate the Traj-Derived ozone in the lower troposphere. After the 1990s, owing to the additional ozonesonde measurements provided by SHADOZ in the tropics, the underestimation of Traj-Derived ozone in the lower troposphere is greatly reduced and the linear fitting coefficient is very close to 1 (and Rs increased to > 0.71). Similarly, with the additional ozonesonde measurements after the 1990s, the Rs in the upper

https://doi.org/10.5194/egusphere-2024-800
Preprint. Discussion started: 2 April 2024

troposphere increased from < 0.50 to > 0.58. In all decades, the agreement between Sonde-Observed and Traj-Derived ozone in the stratosphere is the best, with Rs of ~0.97 and linear coefficients of 0.99. The RD in each decade is small (-0.3% - 1.4%), indicating no systematic underestimation or overestimation in the stratospheric Traj-Derived data. However, in the upper troposphere, Traj-Derived ozone tends to be overestimated, with RD of 0.6-4.5%.

Figure 3 examines how the RD between the ozonesondes and Traj-Derived ozone values varies with altitude, presenting the frequency distributions of RD across all stations, at every other altitude level and in each decade. The distributions of RD show little skewness in every other altitude and decade, indicating no systematic bias during the study period. The overall interquartile ranges (25-75%) of RD are between -30 and 30%, with the lowest interquartile ranges of RD (-10 to 10%) in the stratosphere and middle and lower troposphere. Higher interquartile ranges of RD appear in the 13-19 km altitude range, where the upper troposphere-lower stratosphere (UTLS) region is located, and are due to the large vertical gradients of ozone concentrations in the UTLS and the variability of the tropopause (Millan et al., 2023). The surface (boundary layer) ozone, however, shows a positive bias of the median, in all decades, of up to 12%, suggesting that TOST, which neglects ozone chemistry and deposition, often overestimates ozone concentration there.

Figure 4 exemplifies comparisons in vertical profiles between Sonde-Observed and Traj-Derived ozone profiles at individual stations in different seasons. Four stations with sufficient data coverage (>15 years) were selected from the Antarctic coastal region (Syowa), Europe (Hohenpeissenberg), North America (Boulder), and East Asia (Beijing). The decadal mean (1990s and 2000s) profiles in January and July are used to compare the performance of Traj-Derived ozone profiles in boreal winter and summer. In general, the Traj-Derived profiles can capture the vertical ozone variation in different seasons, with good correlation (R > 0.99) and high accuracy (bias < 100 ppbv, RD < 10%) in comparison to the independent ozonesonde profiles. The Syowa

https://doi.org/10.5194/egusphere-2024-800
Preprint. Discussion started: 2 April 2024

comparison shows a larger bias, but much of this is due to the fact that in the 1990s this station launched the Japanese KC-79 carbon-iodine sonde, while other stations in the Southern Hemisphere launched ECC sondes; the Traj-Derived profiles would therefore be expected to be 10-20% higher in the troposphere and about 5% higher in the lower stratosphere (Smit and Kley, 1998). The excellent agreement in tropospheric ozone at Hohenpeissenberg is likely due to frequent and dense European ozonesonde observations; similar cases also are seen at Uccle, Payerne, and Praha. Larger discrepancies are shown near the planetary boundary layer (PBL) and UTLS, as the simulated trajectories over these regions have more uncertainties (Stohl and Seibert, 1998; Sicard et al., 2019), and ozone chemistry and deposition are potentially important in the PBL at time scales similar to that of the longer trajectories (four days).

3.2 Comparisons with satellite data

To compare with satellite data, we first validated the Traj-Derived ozone profiles against ozonesonde measurements. The corresponding validation was conducted for the satellite data of SAGE and MLS in the same period and location. The sets of ozonesonde, Traj-Derived and satellite data were selected only when all three datasets were available in the same month, decade, and gridpoint, so to ensure that both the Traj-Derived and satellite data could be independently evaluated by the ozonesondes. Figures 5a-d show the vertical RD of the Traj-Derived and SAGE ozone. Compared to SAGE, Traj-Derived ozone concentrations agree with the ozonesondes better in the troposphere (<12 km), with the RD generally < 20%. Above 11 km, Traj-Derived and SAGE ozone concentrations have comparable RD of 10-25% between 12-20 km, and less than 5% above 20 km. In the 12-20 km range, SAGE ozone agrees better with the ozonesondes, particularly in the 1980s.

Figures 5e-h compare the vertical RD of the Traj-Derived and MLS ozone values. The MLS

https://doi.org/10.5194/egusphere-2024-800
Preprint. Discussion started: 2 April 2024

profiles are validated only above the altitude recommended (261 hPa, Livesey et al., 2022). In the lowermost stratosphere, from 12-17 km, MLS shows comparable or better performance than Traj-Derived ozone, while above 17 km the RD of MLS ozone is higher by 0.62-11.88% than that of Traj-Derived ozone, particularly in boreal summer (JJA).

It is of course expected that TOST would outperform satellite instruments in measurements below the tropopause, as satellite measurements are hampered by the large stratospheric ozone burden that satellite instruments must look through, but these comparisons suggest that even above 15 km, where SAGE and MLS are considered most reliable (Wang et al., 2002; Kremser et al., 2020; Livesey et al., 2022), TOST can provide comparable or better accuracy.

Figures 6 show time series of the vertical variation of monthly RD from 16-26 km between Traj-Derived and SAGE ozone from 1985-2005, and between Traj-Derived and MLS ozone from 2005-2019. SAGE ozone data are reliable above 20 km (Kremser et al., 2020), having a mean RD of about -10-10%, similar to that of Traj-Derived ozone. SAGE ozone concentrations are lower than the Traj-Derived ozone by 5 to 10% between 16 and 20 km (Figure 6f), as Traj-Derived ozone overestimates the ozonesondes by 9 to 15% (Figure 6e) while SAGE ozone underestimates the ozonesondes by -7 to -1% (Figure 6d). Over the MLS period from 2005 to 2019, TOST ozone at all altitudes between 16 and 26 km agrees with independent ozonesondes better than during the SAGE period (Figures 6h and 6k vs. Figures 6b and 6e). Accordingly, the Traj-Derived ozone concentrations show good agreement with MLS ozone above 22 km, but are lower than MLS ozone below 20 km (Figures 6i and 6l), as MLS generally overestimates ozone concentrations below 20 km (Figures 6g and 6j).

Figure S4 compares the RMSE of Traj-Derived and satellite ozone in different latitude zones from 16-26 km. Compared to SAGE in the 1990s, the Traj-Derived ozone has comparable RMSEs in the Northern Hemisphere, yet higher RMSEs in the Southern Hemisphere, due to the fewer

https://doi.org/10.5194/egusphere-2024-800
Preprint. Discussion started: 2 April 2024

ozonesonde stations there. MLS ozone also shows lower RMSEs in the Southern Hemisphere, but higher RMSEs in the Northern Hemisphere.

Figure S5 compares monthly average ozone mixing ratios of Traj-Derived ozone with corresponding SAGE and MLS averages, above 16 km, in two seasons. The monthly average values correlate very well, with R = 0.94-0.98, for both instruments and both seasons. Seasonally, Traj-Derived ozone is slightly higher than either SAGE or MLS ozone in DJF (linear fitting slope >1; RD between 1 and 3%), but markedly lower than MLS in JJA (linear fitting slope 0.91-0.92; RD -8 to -9%).

Table S2 summarizes the evaluation of both Traj-Derived and satellite ozone against the ozonesondes over 16-26 km. The Traj-Derived and SAGE ozone values show high correlation (R = 0.95 or greater in all cases), and the Traj-Derived comparison shows RDs of -1% to +2% in the 1980s and 1990s, but only -0.3% to +0.4% in the 2000s and 2010s. By contrast, the SAGE comparison shows RDs of -4% to +0.5%, while the MLS comparison shows RDs of -2% to +11%.

3.3 Comparisons with aircraft observations

We also compare TOST ozone with the IAGOS dataset, in the lower troposphere at 0-50 ppbv, from 1994-2021 (Figure 7). Note that this comparison is between the full TOST (not Traj-derived) and IAGOS datasets here. TOST ozone values are generally higher than IAGOS with a mean bias of 2.2 ppbv and R of 0.49, but RDs (5.8%) and RMS (8.8 ppbv) are low. The linear fit has a slope of 1.03. The two ozone datasets employ different measurement techniques and atmospheric sampling (Petetin et al., 2018). Previous studies have reported that IAGOS ozone values are systematically lower than ozonesonde values, typically by 5-10% in the free troposphere (Tilmes et al., 2012; Zbinden et al., 2013; Staufer et al., 2013, 2014; Tanimoto et al., 2015; Tarasick et al., 2019b). The comparisons in Figure 6 are consistent with these earlier estimates, as the RD (Figure

https://doi.org/10.5194/egusphere-2024-800
Preprint. Discussion started: 2 April 2024

3d) indicates that IAGOS measurements average 6% lower than TOST, with only slight variation (5-8%) when the comparison is made by decade. In the upper troposphere at 6-10 km, however, the IAGOS measurements are on average 12% lower than TOST, with also slight variation (11-12%) between decades (Figure S3).

3.4 Improvements in the new version

The improvements in TOST-v2 are attributed to the increased amount and improved quality of ozonesonde data, as well as the improved trajectory simulation and ozone mapping. Because more ozonesonde stations and more ozonesonde data have become available since the 1990s or 2000s (Table S1), more ozone profiles were used in constructing TOST-2, leading to improved data density. Table S3 summarizes the data coverage, the number of ozonesonde stations and ozonesonde profiles used for TOST-v2 and TOST-v1. The data coverage is defined as the ratio of the number of gridpoints with valid annual means to the total number of gridpoints in the corresponding latitudinal zone. The number of ozonesonde stations, compared to Liu et al. (2013b), increases in all latitudes by ~50%, and the total number of ozonesonde profiles used is doubled. Data coverage increases as well, in all latitude bands, by 5-15% (Table S3) and in all altitudes by a maximum of 10% (Figure S6).

In addition to the data density, the data quality was also improved in TOST-v2. Figure 8a-b shows the distributions of ozone concentrations in TOST-v2 and TOST-v1 at the lowest level (0-1 km) for the 2000s. Over the Antarctic, gaps are observed only in the new TOST data. This is more reasonable for the sea-level data because the altitude over the Antarctic is over 1 km (Figure S7a), where ozone trajectories should not appear at 0-1 km. Therefore, the spatial distributions of ozone are clearly improved with this topography correction in TOST-v2 compared to TOST-v1, which could be attributed to the updated terrain file since HYSPLIT v5.0

https://doi.org/10.5194/egusphere-2024-800
Preprint. Discussion started: 2 April 2024

(https://www.arl.noaa.gov/hysplit/hysplit-model-updates/). Over the eastern Pacific, marked with an ellipse in Figure 8a, b, TOST-v1 shows higher ozone concentrations than TOST-v2 by 30% (Figure 8c). Compared to the ozonesonde measurement at 0-1 km in the 2000s in these two regions (Davis station for the Antarctic and Easter Island station for the eastern Pacific), TOST-v2 agrees better with ozonesondes than TOST-v1, indicating better representation of ozone distributions (Figure S7b).

With reference to spatial distributions at 19-20 km in the 2000s, Figure 8d-e shows that in the Antarctic and the tropical eastern Pacific, TOST-v1 values show higher concentrations than TOST-v2 (Figure 8f). Figure S7c compares ozone concentrations from ozonesonde, TOST-v2, and TOST-v1 at 19-20 km in the 2000s at an Antarctic station (Syowa) and a tropical station (Bogota). Compared to TOST-v1, TOST-v2 ozone values show a better agreement with the ozonesonde measurement. The difference between TOST-v2 ozone and ozonesonde measurements is 10% and 29% in Syowa and Bogota stations, while in TOST-v1, ozone concentrations at these stations show 24% and 39% differences (Figure S7c).

In summary, TOST has been improved in TOST-v2 with higher spatial coverage, improved description of ozone spatial distributions, and a better agreement with ozonesonde measurements in both the troposphere and stratosphere.

3.5 Uncertainty analysis

As noted in Section 2.3, the ozone concentrations in each of the TOST gridpoints (or bins) in a month are determined by the ozone concentrations along all the trajectories passing through that gridpoint in that month. Therefore, an estimate of the random uncertainty of TOST may be obtained from the standard error of the mean in each bin. Note that this may not be a true estimate of the standard error, as some bins may contain more than one value from an individual trajectory,

https://doi.org/10.5194/egusphere-2024-800
Preprint. Discussion started: 2 April 2024

depending on wind speed, and so these values are not independent and our standard error calculation is biased low.

For convenience, given the large range of ozone concentrations between the stratosphere and troposphere, we use the ratio of the standard error to the mean in that bin, SE/Mean, expressed in %. The standard error is proportional to the variability of the ozone values in a bin (i.e. the standard deviation) and inversely proportional to the square root of the number of data values. Thus in general, the more trajectories passing a gridpoint, the more data points for that gridpoint and the lower the standard error for that gridpoint. Figure 9 shows the SE/Mean and the number of samples in January and July of the 2000s at 3-4 km and 19-20 km. Generally, the Southern Hemisphere shows higher SE/Mean values (> 10%) than the Northern Hemisphere (< 6%), which reflects the large number (>100) of ozone soundings in the Northern Hemisphere, especially over North America and Europe. However, near the equator, despite the higher sampling rate, the SE/Mean still is as high as 15%. Compared to the stratospheric level (19-20 km), the tropospheric level (3-4 km) shows an overall higher SE/Mean. SE/Mean varies less with season in the stratosphere than in the troposphere. For example, at 3-4 km, the SE/Mean in January is generally <7% but becomes >10% in July in the Northern Hemisphere, and vice versa in the Southern Hemisphere. This is likely due to more vertical motion in the PBL (Stohl and Seibert, 1998; Sicard et al., 2019) so that ozone in some bins comes from multiple altitude levels, as well as increased photochemistry and biomass burning. Stratospheric intrusions to the lower troposphere are more frequent in boreal spring and summer than in winter (Terao et al., 2008; Greenslade et al., 2017), and can be responsible for much of the variability at 3-4 km (Tarasick et al., 2019a).

To quantify the uncertainties of TOST ozone in different altitudinal and latitudinal zones, and in different seasons and decades, we calculated the Normalized Root Mean Squared Error (NRMSE) of the monthly ozone mixing ratio between ozonesonde and Traj-Derived ozone over

https://doi.org/10.5194/egusphere-2024-800
Preprint. Discussion started: 2 April 2024

1970-2021 (Figure 10). Among altitudes, the highest NRMSE values appear at 9-10 km and over the tropopause region, and the second highest NRMSE at the surface, while the lowest NRMSE values are in the lower to middle troposphere (3-6 km) and stratosphere (19-26 km), consistent with Figure 4. There is considerable variation in NRMSE with latitude; the NRMSEs in the southern high latitudes (90-60S) and the northern tropics (0-30N) are higher than in other latitudinal zones. This could reflect higher horizontal gradients of ozone (e.g. stations in or outside the ozone hole) in the southern high latitudes or biases between ECC sondes and other types (the Indian and Japanese sondes) in the northern tropics. By season, the NRMSE varies slightly with a lower value in March-April-May than in other seasons. After the 1990s, the NRMSEs are reduced markedly compared to the 1980s and 1970s, likely related to the improved data coverage in the later period. This overview provides caveats regarding where (surface and UTLS, the northern high latitudes and tropics) and when (before the 1990s) more caution is advised when using TOST.

4. Global ozone spatial-temporal variations observed from TOST

4.1 Ozone spatial variations in the troposphere and stratosphere

As a 3-dimensional ozone dataset, TOST can depict both horizontal and vertical ozone distributions, as well as long-term ozone timeseries. Figure 11 shows distributions of decadal mean TOST ozone at 3-4 km and 19-20 km in four seasons of the 2000s. At 3-4 km in the troposphere, ozone concentrations are higher over the continent in the Northern Hemisphere, especially in MAM and DJF (>50 ppbv), reflecting the ozone production from the photochemical reactions of anthropogenic and natural emissions. In addition, the continental outflow from the southern US (in MAM) and the biomass burning-produced ozone in southern Africa (in JJA and SON) are well captured and in agreement with satellite observations (Fishman et al., 1990; Ebojie et al., 2016). At 19-20 km in the stratosphere (Figure 11e-h), ozone concentrations are higher near the poles

https://doi.org/10.5194/egusphere-2024-800
Preprint. Discussion started: 2 April 2024

than in the tropics, due to the impact of the Brewer–Dobson circulation. The North Pole has higher ozone concentrations than the South Pole in DJF and MAM, and vice versa in JJA and SON, reflecting the seasonality of the Brewer-Dobson circulation. Also at 19-20 km, the ozone concentrations are lower over Asia in JJA (Figure 11f) than in other seasons, reflecting the transport of ozone by Asian summer monsoon from the tropics (Gettelman et al., 2004; Bian et al., 2020).

Although trajectory mapping fills in much of the spatial domain, large gaps can still be found, particularly in the tropics, where ozone soundings are less dense. Since some applications require a default ozone value at all gridpoints, a smoothed ozone dataset is also provided for the decadal mean ozone in each month and the annual mean ozone, by fitting the maps at each level to a linear combination of spherical functions (Liu et al., 2013b). As shown in Figures 11i-p, small-scale variations and extreme values are reduced in the smoothed ozone fields, while broad patterns of the ozone distribution are retained, making these smoothed maps valuable for qualitative visualization of the spatial, seasonal, and decadal variations in ozone at different altitudes. They should, however, be used for any kind of quantitative analysis with great caution, as these highly interpolated data, where gaps exist in the unsmoothed TOST dataset, are necessarily far from any original measurement and the degree to which they represent the true ozone value is doubtful. For example, erroneous conclusions have been inferred from the smoothed TOST-v1 output over the tropics, with very limited observations before 1998, where the smoothed data were mostly interpolated from higher latitudes (Chipperfield et al., 2022). In addition, smoothing, as noted, removes small-scale variations and extreme values, and does so whether they are real or not. The smoothed dataset has not been quantitatively evaluated in any way.

Figure 12a-d shows the latitude-altitude distribution of TOST ozone in each season averaged over 1970-2021. The steep changes in ozone concentration from <100 to >500 ppbv in the vicinity

https://doi.org/10.5194/egusphere-2024-800
Preprint. Discussion started: 2 April 2024

of the tropopause (the black lines in Figure 12a-d, calculated from the NCEP/NCAR reanalysis) are well captured. Due to the Brewer-Dobson circulation, ozone concentrations above the tropopause increase with latitude from the tropics to the poles, which is also well reflected in the latitude-altitude distribution. TOST ozone concentrations are higher in spring (600-800 ppbv) than in the other seasons (< 500 ppbv) over northern midlatitudes (45-60°N) at about 12-13 km, which reflects the stronger Brewer-Dobson circulation in spring (Holton et al., 1995). Figure 12e shows the monthly mean TOST ozone time series from 1970 to 2021, averaged over 30-70°N at each level. Clear seasonal cycles are well captured every year.

4.2 Long-term trend in stratospheric ozone

One of the advantages of TOST is its long-term coverage, which enables investigation of variations in ozone back to the 1970s. One application is to study stratospheric ozone changes, as it is important to assess stratospheric ozone recovery (or lack thereof) since the implementation of the Montreal Protocol and its amendments (Fang et al., 2019). While this is commonly done with individual ozonesonde time series, it is challenging to assess how well individual long-term station changes represent regional or global variations. Combining data records from sparse and widely separated ozonesonde sites involves implicit assumptions about their representativeness. With meteorological trajectory mapping, each original ozonesonde measurement is assigned a trajectory which describes its representativeness, and the TOST averages are therefore weighted according to the representativeness of each measurement. While this is subject to trajectory errors and the fact that coverage is incomplete (Table S3), unless trajectory errors are non-random, it should produce a better result than simple averaging of sonde station data by geographic region.

Figure 13 shows the area-weighted annual averages of ozone concentrations at 21-22 km and 24-25 km from 1970 to 2021; averages were taken over all gridpoints from 30°-70°N with

https://doi.org/10.5194/egusphere-2024-800
Preprint. Discussion started: 2 April 2024

available data throughout all years (~ 70% of gridpoints). The 3-year running means are also shown with the time series. The ozone time series at both levels captures the ozone depletion in the early 1990s from the effects of the 1991 eruption of Mt. Pinatubo (McCormick et al., 1995; Tang et al., 2013; Dhomse, et al., 2015) and the recovery in the latter part of the 1990s. In addition, these updated TOST time series show that stratospheric ozone since 2000 changed little, despite the decline in stratospheric chlorine since then. From Figure 14, there is an insignificant trend in the ozone concentrations at 21-22 km (by 0.6 ppbv/year) and 24-25 km (by -1.9 ppbv/year) from 1998 to 2021, indicating little change of stratospheric ozone, despite the fact that 25 years have passed since peak stratospheric chlorine. Using long-term satellite data, Bognar et al. (2022) also find stratospheric ozone largely unchanged in the last two decades, which, they suggest, is related to asymmetries and long-term variability in the Brewer-Dobson circulation. Such observations of the variation in stratospheric ozone are essential to verifying the expected stratospheric ozone recovery under the Montreal Protocol.

5. Conclusions

An improved TOST dataset has been generated from 1970 to 2021 based on the updated ozonesonde profiles at 141 ozonesonde stations from WOUDC, SHADOZ, HEGIFTOM and NDACC. The updated TOST was derived by combining the 4-day forward and backward trajectories from each ozonesonde profile, which were driven by the most state-of-the-art HYSPLIT model (v5.2) and NCEP reanalysis data (NNRP-1). The monthly mean ozone, decadal mean ozone in each month (January to December from the 1970s-2010s) and annual mean ozone (1970-2021) are provided in 3-dimensional grids of 5º × 5º × 1 km (latitude, longitude, and altitude). Spatially-smoothed maps are also provided by decadal mean in each month and annual mean for qualitative visualization, model initialization, and other applications with caution. For

https://doi.org/10.5194/egusphere-2024-800
Preprint. Discussion started: 2 April 2024

user convenience, the TOST data in coordinates from the sea level and from the surface level are both generated, and separate ozone climatology datasets are generated based on trajectories from ozonesonde in both the troposphere and stratosphere, trajectories from ozonesonde only in the troposphere and trajectories from ozonesonde only in the stratosphere. Statistics (standard error, number of samples) are also provided.

Comprehensive validation of TOST-v2 was conducted. At all the ozonesonde stations used, trajectory-derived ozone profiles without the input of the station itself were compared with the corresponding ozonesonde profiles at the stations. The overall comparison between the ozonesonde and trajectory-derived ozone shows good agreement in both the troposphere (R = 0.56-0.69, RD = 2-4%) and stratosphere (R = 0.97, RD = 0.5%) in each decade and in all decades' mean (Figure 2). The frequency distribution of RD at different altitudes shows interquartile ranges of RD between -30 to 30%, with the lowest interquartile ranges of RD (-10 to 10%) in the stratosphere and lower troposphere, and no systematic bias except in the surface layer (Figure 3). The patterns of ozone profiles at individual stations are also well captured and quantified, with $R > 0.76$ and RD of 2-8% (Figure 4). Larger discrepancies are shown near the PBL and UTLS, especially for coastal stations where the trajectory-derived ozone may be biased by trajectories from the continent (Tarasick et al., 2010).

The comparison between TOST and satellite data, i.e., SAGE in the 1980s and 1990s, and MLS in the 2000s and 2010s, illustrates that TOST data have comparable accuracy with the satellite data in the stratosphere, while in the troposphere TOST is markedly superior (Figure 5). In different latitude zones and decades, TOST performs comparably with SAGE and MLS data as well (Figure 6). TOST-v2 was also directly compared to MOZAIC-IAGOS ozone profiles over the period 1994-2021 from the surface to 5 km. Despite the systematic difference between MOZAIC-IAGOS and ozonesonde measurements, the two ozone datasets agree well in each decade and in

https://doi.org/10.5194/egusphere-2024-800
Preprint. Discussion started: 2 April 2024

all decades' mean for lower troposphere (RD =5-8%, Figure 7) and upper troposphere (RD =11-12%, Figure S3).

Compared to the previous version of TOST (TOST-v1, Liu et al. 2013a and b), this new TOST, TOST-v2, is improved in two major aspects. Firstly, the record is extended to 2021 and data coverage is increased by as much as 15%, as more ozone profiles and 43 additional ozonesonde stations are used in constructing the new version of TOST. Secondly, the spatial distribution of ozone has better agreement with ozonesonde measurements in both the troposphere and stratosphere over regions of Antarctica and the eastern Pacific, with RD decreased by > 50%. The uncertainties of TOST are largely dependent on the availability of ozonesonde data. Higher uncertainties are found before the 1990s, as global coverage is sparse in the tropics before SHADOZ. Higher uncertainties also appear at southern high latitudes and in the northern tropics, with NRMSE there being 35-78% higher than at northern midlatitudes (Figure 10), likely because of greater ozone variability there, although biases between ozonesonde types may also contribute. TOST data at the PBL and UTLS have higher standard error and twice the NRMSE compared to other altitude levels; the former is due to more small-scale processes in the PBL while the latter is related to the large ozone gradient and the dynamic variation of the tropopause.

TOST can capture global ozone distributions in the troposphere and stratosphere (Figures 11 and 12), showing horizontal and vertical variations, the continental outflow, and the gradient of ozone concentration near the tropopause. TOST can also reflect the seasonal variations in ozone concentrations near the vicinity of the tropopause. The time series of the updated TOST shows the stagnant recovery but overall insignificant change of stratospheric ozone after 1998 (Figure 13), which agrees well with studies using satellite-based and model-based ozone datasets (Bognar et al., 2022).

It is anticipated that this updated and improved TOST dataset can benefit future studies, owing

https://doi.org/10.5194/egusphere-2024-800
Preprint. Discussion started: 2 April 2024

to its long record, global coverage, and high vertical resolution. We expect that it will be a useful dataset for trend studies, especially in the free troposphere, and also in the stratosphere, given the excellent long-term stability of the global ozonesonde network (Stauffer et al., 2022). We caution, however, that users should keep in mind the assumptions and limitations of the data product as described here.

Author contribution

J. L. and D.T. conceptualized and designed this study. Z.Z. performed data process, analysis, and composed the first draft. All the coauthors contributed substantially to this study in making ozonesonde measurements, processing, calibrating, and archiving the ozonesonde data, and providing constructive and valuable suggestions to and comments on the manuscript. All the co-authors approved the submission of this paper.

Code and data availability

The ozonesonde data used in this study can be obtained from the WOUDC (https://woudc.org/archive/Archive-NewFormat/OzoneSonde_1.0_1/), SHADOZ (https://doi.org/10.57721/SHADOZ-V06) and HEGIFTOM (https://hegiftom.meteo.be/datasets/ozonesondes). The trajectory model HYSPLIT (Version 5.2) is from the NOAA Air Resources Laboratory (http://www.arl.noaa.gov/ready.html), driven by the NCEP/NCAR reanalysis data from the NOAA/OAR/ESRL PSD, Boulder, Colorado, USA, at https://www.ready.noaa.gov/data/archives/reanalysis/. The aircraft data can be accessed from IAGOS network (https://www.iagos.org/). The two satellite data for comparison, the SAGE II (Version 7.0) and the MLS (Version 5.0), are obtained from https://sage.nasa.gov/missions/about-sage-ii/ and https://disc.gsfc.nasa.gov/datasets/ML2O3_005/summary?keywords=ML2O3_005, respectively.

https://doi.org/10.5194/egusphere-2024-800
Preprint. Discussion started: 2 April 2024

We are in the process of making the TOST available at the WOUDC website. TOST data currently are available on request from the authors.

Competing interests

The authors declare that they have no conflict of interest.

Special issue statement

This article is part of the special issue "Tropospheric Ozone Assessment Report Phase II (TOAR-II) Community Special Issue (ACP/AMT/BG/GMD inter-journal SI)".

Acknowledgements

We thank many for their dedication to WOUDC, SHADOZ, and HEGIFTOM, making ozonesonde data accessible. We also thank SAGE II and MLS team for their ozone data for comparison. We acknowledge the HYSPLIT team for the trajectory model. Z. Z. and J. L. acknowledge the financial support from Natural Science and Engineering Council of Canada (Grant No. RGPIN-2020-05163); J. B. and J. Z. from the National Natural Science Foundation of China (Grant No. 42293321).

References

Ancellet, G., Godin-Beekmann, S., Smit, H. G., Stauffer, R. M., Van Malderen, R., Bodichon, R., and Pazmiño, A.: Homogenization of the Observatoire de Haute Provence electrochemical concentration cell (ECC) ozonesonde data record: comparison with lidar and satellite observations, Atmospheric Measurement Techniques, 15, 3105-3120, 2022.

Badia, A., Iglesias-Suarez, F., Fernandez, R. P., Cuevas, C. A., Kinnison, D. E., Lamarque, J. F., Griffiths, P. T., Tarasick, D. W., Liu, J., and Saiz-Lopez, A.: The role of natural halogens in global tropospheric ozone chemistry and budget under different 21st century climate scenarios, Journal of Geophysical Research: Atmospheres, 126, e2021JD034859, 2021.

Bhartia, P. K.: OMI Algorithm Theoretical Basis Document Volume II, OMI Ozone, 2002.

Bian, J., Gettelman, A., Chen, H., and Pan, L. L.: Validation of satellite ozone profile retrievals using Beijing ozonesonde data, Journal of Geophysical Research: Atmospheres, 112, 2007.

Bian, J., Li, D., Bai, Z., Li, Q., Lyu, D., and Zhou, X.: Transport of Asian surface pollutants to the global stratosphere from the Tibetan Plateau region during the Asian summer monsoon, National Science Review, 7, 516-533, 2020.

Bodeker, G. E., Nitzbon, J., Tradowsky, J. S., Kremser, S., Schwertheim, A., and Lewis, J.: A global total column ozone climate data record, Earth System Science Data, 13, 3885-3906, 2021.

Bognar, K., Tegtmeier, S., Bourassa, A., Roth, C., Warnock, T., Zawada, D., and Degenstein, D.: Stratospheric ozone trends for 1984–2021 in the SAGE II–OSIRIS–SAGE III/ISS composite dataset, Atmospheric Chemistry and Physics, 22, 9553-9569, 2022.

Chen, X., Liu, Y., Lai, A., Han, S., Fan, Q., Wang, X., Ling, Z., Huang, F., and Fan, S.: Factors dominating 3-dimensional ozone distribution during high tropospheric ozone period, Environmental Pollution, 232, 55-64, 2018.

Chipperfield, M. P., Chrysanthou, A., Damadeo, R., Dameris, M., Dhomse, S. S., Fioletov, V., Frith, S. M., Godin-Beekmann, S., Hassler, B., and Liu, J.: Comment on "Observation of large and all-season ozone losses over the tropics" [AIP Adv. 12, 075006 (2022)], AIP Advances, 12, 2022.

Cunnold, D., Wang, H., Chu, W., and Froidevaux, L.: Comparisons between Stratospheric Aerosol and Gas Experiment II and microwave limb sounder ozone measurements and aliasing of SAGE II ozone trends in the lower stratosphere, Journal of Geophysical Research: Atmospheres, 101, 10061-10075, 1996.

Dhomse, SS, MP Chipperfield, W Feng, R Hossaini, GW Mann, and ML Santee, Revisiting the hemispheric asymmetry in midlatitude ozone changes following the Mount Pinatubo eruption: A 3-D model study. Geophysical Research Letters, 42, 3038–3047, 2015.

Draxler, R. R. and Hess, G.: An overview of the HYSPLIT_4 modelling system for trajectories, Australian meteorological magazine, 47, 295-308, 1998.

Ebojie, F., Burrows, J., Gebhardt, C., Ladstätter-Weißenmayer, A., Von Savigny, C., Rozanov, A., Weber, M., and Bovensmann, H.: Global tropospheric ozone variations from 2003 to 2011 as

https://doi.org/10.5194/egusphere-2024-800
Preprint. Discussion started: 2 April 2024

seen by SCIAMACHY, Atmospheric Chemistry and Physics, 16, 417-436, 2016.
Engström, A. and Magnusson, L.: Estimating trajectory uncertainties due to flow dependent errors in the atmospheric analysis, Atmospheric Chemistry and Physics, 9, 8857-8867, 2009.
Eyring, V., Cionni, I., Bodeker, G. E., Charlton-Perez, A. J., Kinnison, D. E., Scinocca, J. F., Waugh, D. W., Akiyoshi, H., Bekki, S., and Chipperfield, M. P.: Multi-model assessment of stratospheric ozone return dates and ozone recovery in CCMVal-2 models, Atmospheric Chemistry and Physics, 10, 9451-9472, 2010.
Fang, X., Pyle, J. A., Chipperfield, M. P., Daniel, J. S., Park, S., and Prinn, R. G.: Challenges for the recovery of the ozone layer, Nature Geoscience, 12, 592-596, 2019.
Fioletov, V., Tarasick, D., and Petropavlovskikh, I.: Estimating ozone variability and instrument uncertainties from SBUV (/2), ozonesonde, Umkehr, and SAGE II measurements: Short-term variations, Journal of Geophysical Research: Atmospheres, 111, 2006.
Fishman, J., Watson, C. E., Larsen, J. C., and Logan, J. A.: Distribution of tropospheric ozone determined from satellite data, Journal of Geophysical Research: Atmospheres, 95, 3599-3617, 1990.
Gaudel, A., Cooper, O. R., Ancellet, G., Barret, B., Boynard, A., Burrows, J. P., Clerbaux, C., Coheur, P.-F., Cuesta, J., and Cuevas, E.: Tropospheric Ozone Assessment Report: Present-day distribution and trends of tropospheric ozone relevant to climate and global atmospheric chemistry model evaluation, Elementa: Science of the Anthropocene, 6, 2018.
Gettelman, A., Kinnison, D. E., Dunkerton, T. J., and Brasseur, G. P.: Impact of monsoon circulations on the upper troposphere and lower stratosphere, Journal of Geophysical Research: Atmospheres, 109, 2004.
Greenslade, J. W., Alexander, S. P., Schofield, R., Fisher, J. A., and Klekociuk, A. K.: Stratospheric ozone intrusion events and their impacts on tropospheric ozone in the Southern Hemisphere, Atmospheric Chemistry and Physics, 17, 10269-10290, 2017.
Griffiths, P. T., Murray, L. T., Zeng, G., Shin, Y. M., Abraham, N. L., Archibald, A. T., Deushi, M., Emmons, L. K., Galbally, I. E., Hassler, B. L.W. Horowitz, J. Keeble, J. Liu, O. Moeini, V. Naik, F.M. O'Connor, D. Tarasick, S. Tilmes, S.T. Turnock, O. Wild, P.J. Young and P. Zanis: Tropospheric ozone in CMIP6 simulations, Atmospheric Chemistry and Physics, 21, 4187-4218, 2021.
Gulev, S. K., Thorne, P. W., Ahn, J., Dentener, F. J., Domingues, C. M., Gerland, S., Gong, D.,

https://doi.org/10.5194/egusphere-2024-800
Preprint. Discussion started: 2 April 2024

Kaufman, D. S., Nnamchi, H. C., and Quaas, J.: Changing state of the climate system, 2021.

Hassler, B., Bodeker, G., and Dameris, M.: A new global database of trace gases and aerosols from multiple sources of high vertical resolution measurements, Atmospheric Chemistry and Physics, 8, 5403-5421, 2008.

Hassler, B., Kremser, S., Bodeker, G. E., Lewis, J., Nesbit, K., Davis, S. M., Chipperfield, M. P., Dhomse, S. S., and Dameris, M.: An updated version of a gap-free monthly mean zonal mean ozone database, Earth System Science Data, 10, 1473-1490, 2018.

Holton, J. R., Haynes, P. H., McIntyre, M. E., Douglass, A. R., Rood, R. B., and Pfister, L.: Stratosphere-troposphere exchange, Reviews of Geophysics, 33, 403-439, 1995.

Jacob, D. J.: Introduction to atmospheric chemistry, Princeton University Press, 1999.

Kalney, E., Kanamitsu, M., Kistler, R., Collins, W., Deaven, D., Gandin, L., Iredell, M., Saha, S., White, G., Woollen, J., Zhu, Y., Chelliah, M., Ebisuzaki, W., Higgins, W., Janowiak, J., Mo, K. C., Ropelewski, C., Wang, J., Leetmaa, A., Reynolds, R., Jenne, R., and Joseph, D.: The NCEP/NCAR 40-Year Reanalysis Project, Bulletin of the American Meteorological Society, 77, 437-472, 1996.

Kent, G., Winker, D., Osborn, M., and Skeens, K.: A model for the separation of cloud and aerosol in SAGE II occultation data, Journal of Geophysical Research: Atmospheres, 98, 20725-20735, 1993.

Kremser, S., Thomason, L. W., and Bird, L. J.: Simplified SAGE II ozone data usage rules, Earth System Science Data, 12, 1419-1435, 2020.

Liu, G., Tarasick, D. W., Fioletov, V. E., Sioris, C. E., and Rochon, Y. J.: Ozone correlation lengths and measurement uncertainties from analysis of historical ozonesonde data in North America and Europe, Journal of Geophysical Research: Atmospheres, 114, 2009.

Liu, G., Liu, J., Tarasick, D., Fioletov, V., Jin, J., Moeini, O., Liu, X., Sioris, C., and Osman, M.: A global tropospheric ozone climatology from trajectory-mapped ozone soundings, Atmospheric Chemistry and Physics, 13, 10659-10675, 2013a.

Liu, J., Tarasick, D., Fioletov, V., McLinden, C., Zhao, T., Gong, S., Sioris, C., Jin, J., Liu, G., and Moeini, O.: A global ozone climatology from ozone soundings via trajectory mapping: a stratospheric perspective, Atmospheric Chemistry and Physics, 13, 11441-11464, 2013b.

Liu, X., Bhartia, P., Chance, K., Spurr, R., and Kurosu, T.: Ozone profile retrievals from the Ozone Monitoring Instrument, Atmospheric Chemistry and Physics, 10, 2521-2537, 2010.

https://doi.org/10.5194/egusphere-2024-800
Preprint. Discussion started: 2 April 2024

Livesey, N., Read, W., Wagner, P., Froidevaux, L., Santee, M., Schwartz, M., Lambert, A., Millán Valle, L., Pumphrey, H., and Manney, G.: Earth Observing System (EOS) Aura Microwave Limb Sounder (MLS) version 5.0 x level 2 and 3 data quality and description document Version 5.0–1.1 a (Tech. Rep.), Jet Propulsion Laboratory, California Institute of Technology. Retrieved from https://mls. jpl. nasa. gov/data/v5-0_data_quality_document. pdf, 2022.

McCormick, J. P., L. W. Thomason, and C. R. Trepte (1995), Atmospheric effects of the Mt. Pinatubo eruption, Nature, 373, 399–404.

McPeters, R. D. and Labow, G. J.: Climatology 2011: An MLS and sonde derived ozone climatology for satellite retrieval algorithms, Journal of Geophysical Research: Atmospheres, 117, 2012.

McPeters, R. D., Labow, G. J., and Logan, J. A.: Ozone climatological profiles for satellite retrieval algorithms, Journal of Geophysical Research: Atmospheres, 112, 2007.

Millan, L. F., Manney, G. L., Boenisch, H., Hegglin, M. I., Hoor, P., Kunkel, D., Leblanc, T., Petropavlovskikh, I., Walker, K., and Wargan, K.: A Multi-Parameter Dynamical Diagnostics for Upper Tropospheric and Lower Stratospheric Studies, EGUsphere, 1-41, 2023.

Moeini, O., Tarasick, D. W., McElroy, C. T., Liu, J., Osman, M. K., Thompson, A. M., Parrington, M., Palmer, P. I., Johnson, B., and Oltmans, S. J.: Estimating wildfire-generated ozone over North America using ozonesonde profiles and a differential back trajectory technique, Atmospheric Environment: X, 7, 100078, 2020.

Nédélec, P., Blot, R., Boulanger, D., Athier, G., Cousin, J.-M., Gautron, B., Petzold, A., Volz-Thomas, A., and Thouret, V.: Instrumentation on commercial aircraft for monitoring the atmospheric composition on a global scale: the IAGOS system, technical overview of ozone and carbon monoxide measurements, Tellus B: Chemical and Physical Meteorology, 67, 27791, 2015.

Nowack, P. J., Luke Abraham, N., Maycock, A. C., Braesicke, P., Gregory, J. M., Joshi, M. M., Osprey, A., and Pyle, J. A.: A large ozone-circulation feedback and its implications for global warming assessments, Nature Climate Change, 5, 41-45, 2015.

Petetin, H., Sauvage, B., Smit, H. G., Gheusi, F., Lohou, F., Blot, R., Clark, H., Athier, G., Boulanger, D., and Cousin, J.-M.: A climatological view of the vertical stratification of RH, O3 and CO within the PBL and at the interface with free troposphere as seen by IAGOS aircraft and ozonesondes at northern mid-latitudes over 1994–2016, Atmospheric Chemistry

https://doi.org/10.5194/egusphere-2024-800
Preprint. Discussion started: 2 April 2024

and Physics, 18, 9561-9581, 2018.

Petzold, A., Thouret, V., Gerbig, C., Zahn, A., Brenninkmeijer, C. A., Gallagher, M., Hermann, M., Pontaud, M., Ziereis, H., and Boulanger, D.: Global-scale atmosphere monitoring by in-service aircraft–current achievements and future prospects of the European Research Infrastructure IAGOS, Tellus B: Chemical and Physical Meteorology, 67, 28452, 2015.

Polvani, L. M., Wang, L., Aquila, V., and Waugh, D. W.: The impact of ozone-depleting substances on tropical upwelling, as revealed by the absence of lower-stratospheric cooling since the late 1990s, Journal of Climate, 30, 2523-2534, 2017.

Sicard, M., Granados-Muñoz, M. J., Alados-Arboledas, L., Barragán, R., Bedoya-Velásquez, A. E., Benavent-Oltra, J. A., Bortoli, D., Comerón, A., Córdoba-Jabonero, C., and Costa, M. J.: Ground/space, passive/active remote sensing observations coupled with particle dispersion modelling to understand the inter-continental transport of wildfire smoke plumes, Remote Sensing of Environment, 232, 111294, 2019.

Skeie, R. B., Myhre, G., Hodnebrog, Ø., Cameron-Smith, P. J., Deushi, M., Hegglin, M. I., Horowitz, L. W., Kramer, R. J., Michou, M., and Mills, M. J.: Historical total ozone radiative forcing derived from CMIP6 simulations, Npj Climate and Atmospheric Science, 3, 32, 2020.

Smit, H. G. and Kley, D.: JOSIE: The 1996 WMO International intercomparison of ozonesondes under quasi flight conditions in the environmental simulation chamber at Jülich, Proceedings of the XVIII Quadrennial Ozone Symposium, 971-974, 1998.

Smit, H. and Thompson, A.: Ozonesonde Measurement Principles and Best Operational Practices: ASOPOS 2.0 (Assessment of Standard Operating Procedures for Ozonesondes), WMO, World Meteorological Organization, GAW Report, 173, 2021.

Staufer, J., Staehelin, J., Stübi, R., Peter, T., Tummon, F., and Thouret, V.: Trajectory matching of ozonesondes and MOZAIC measurements in the UTLS – Part 1: Method description and application at Payerne, Switzerland, Atmospheric Measurement Techniques., 6, 3393-3406, 10.5194/amt-6-3393-2013, 2013.

Staufer, J., Stähelin, J., Stübi, R., Peter, T., Tummon, F., and Thouret, V.: Trajectory matching of ozonesondes and MOZAIC measurements in the UTLS–Part 2: Application to the global ozonesonde network, Atmospheric Measurement Techniques, 7, 241-266, 2014.

Stauffer, R. M., Thompson, A. M., Kollonige, D. E., Tarasick, D. W., Van Malderen, R., Smit, H. G., Vömel, H., Morris, G. A., Johnson, B. J., and Cullis, P. D.: An examination of the recent

https://doi.org/10.5194/egusphere-2024-800
Preprint. Discussion started: 2 April 2024

stability of ozonesonde global network data, Earth and Space Science, 9, e2022EA002459, 2022.

Stauffer, R. M., Thompson, A. M., Kollonige, D. E., Witte, J. C., Tarasick, D. W., Davies, J., Vömel, H., Morris, G. A., Van Malderen, R., and Johnson, B. J.: A post-2013 dropoff in total ozone at a third of global ozonesonde stations: Electrochemical concentration cell instrument artifacts? Geophysical Research Letters, 47, e2019GL086791, 2020.

Stein, A., Draxler, R. R., Rolph, G. D., Stunder, B. J., Cohen, M., and Ngan, F.: NOAA's HYSPLIT atmospheric transport and dispersion modeling system, Bulletin of the American Meteorological Society, 96, 2059-2077, 2015.

Steinbrecht, W., Froidevaux, L., Fuller, R., Wang, R., Anderson, J., Roth, C., Bourassa, A., Degenstein, D., Damadeo, R., and Zawodny, J.: An update on ozone profile trends for the period 2000 to 2016, Atmospheric Chemistry and Physics, 17, 10675-10690, 2017.

Sterling, C. W., Johnson, B. J., Oltmans, S. J., Smit, H. G., Jordan, A. F., Cullis, P. D., Hall, E. G., Thompson, A. M., and Witte, J. C.: Homogenizing and estimating the uncertainty in NOAA's long-term vertical ozone profile records measured with the electrochemical concentration cell ozonesonde, Atmospheric Measurement Techniques, 11, 3661-3687, 2018.

Stohl, A.: Computation, accuracy and applications of trajectories—A review and bibliography, Atmospheric Environment, 32, 947-966, 1998.

Stohl, A., Eckhardt, S., Forster, C., James, P., Spichtinger, N., and Seibert, P.: A replacement for simple back trajectory calculations in the interpretation of atmospheric trace substance measurements, Atmospheric Environment, 36, 4635-4648, 2002.

Stohl, A., James, P., Forster, C., Spichtinger, N., Marenco, A., Thouret, V., and Smit, H. G.: An extension of Measurement of Ozone and Water Vapour by Airbus In-service Aircraft (MOZAIC) ozone climatologies using trajectory statistics, Journal of Geophysical Research: Atmospheres, 106, 27757-27768, 2001.

Stohl, A. and Seibert, P.: Accuracy of trajectories as determined from the conservation of meteorological tracers, Quarterly Journal of the Royal Meteorological Society, 124, 1465-1484, 1998.

Tang, Q., P. G. Hess, B. Brown-Steiner, and D. E. Kinnison, Tropospheric ozone decrease due to the Mount Pinatubo eruption: Reduced stratospheric influx, Geophysical Research Letters, 40, 5553–5558, 2013.

Tanimoto, H., Zbinden, R. M., Thouret, V., and Nédélec, P.: Consistency of tropospheric ozone observations made by different platforms and techniques in the global databases, Tellus B: Chemical and Physical Meteorology, 67, 27073, 2015.

Tarasick, D., Carey-Smith, T., Hocking, W., Moeini, O., He, H., Liu, J., Osman, M., Thompson, A., Johnson, B., and Oltmans, S.: Quantifying stratosphere-troposphere transport of ozone using balloon-borne ozonesondes, radar windprofilers and trajectory models, Atmospheric Environment, 198, 496-509, 2019a.

Tarasick, D., Jin, J., Fioletov, V., Liu, G., Thompson, A., Oltmans, S., Liu, J., Sioris, C., Liu, X., and Cooper, O.: High-resolution tropospheric ozone fields for INTEX and ARCTAS from IONS ozonesondes, Journal of Geophysical Research: Atmospheres, 115, 2010.

Tarasick, D.W., I. Galbally, O.R. Cooper, M.G. Schultz, G. Ancellet, T. LeBlanc, T.J. Wallington, J. Ziemke, X. Liu, M. Steinbacher, J. Stähelin, C. Vigouroux, J. Hannigan, O. García, G. Foret, P. Zanis, E. Weatherhead, I. Petropavlovskikh, H. Worden, J.L. Neu, M. Osman, J. Liu, M. Lin, M. Granados-Muñoz, A.M. Thompson, S.J. Oltmans, J. Cuesta, G. Dufour, V. Thouret, B. Hassler, A.M. Thompson and T. Trickl, TOAR- Observations: Tropospheric ozone from 1877 to 2016, observed levels, trends and uncertainties, Elementa: Science of the Anthropocene, 7(1), p.39, 2019b.

Tarasick, D.W., J. Davies, H.G.J. Smit and S.J. Oltmans, A re-evaluated Canadian ozonesonde record: measurements of the vertical distribution of ozone over Canada from 1966 to 2013, Atmospheric Measurement Techniques, 9, 195-214, 2016.

Tarasick, D.W., H.G.J. Smit, A.M. Thompson G.A. Morris, J.C. Witte, J. Davies, T. Nakano, R. van Malderen, R.M. Stauffer, T. Deshler, B.J. Johnson, R. Stübi, S.J. Oltmans and H. Vömel, Improving ECC ozonesonde data quality: Assessment of current methods and outstanding issues. Earth and Space Science, 8, e2019EA000914, 2021.

Terao, Y., Logan, J. A., Douglass, A. R., and Stolarski, R. S.: Contribution of stratospheric ozone to the interannual variability of tropospheric ozone in the northern extratropics, Journal of Geophysical Research: Atmospheres, 113, 2008.

Thompson, A. M., Witte, J. C., Sterling, C., Jordan, A., Johnson, B. J., Oltmans, S. J., Fujiwara, M., Vömel, H., Allaart, M., and Piters, A.: First reprocessing of Southern Hemisphere Additional Ozonesondes (SHADOZ) ozone profiles (1998–2016): 2. Comparisons with satellites and ground-based instruments, Journal of Geophysical Research: Atmospheres, 122,

https://doi.org/10.5194/egusphere-2024-800
Preprint. Discussion started: 2 April 2024

13,000-013,025, 2017.

Thouret, V., Marenco, A., Logan, J. A., Nédélec, P., and Grouhel, C.: Comparisons of ozone measurements from the MOZAIC airborne program and the ozone sounding network at eight locations, Journal of Geophysical Research: Atmospheres, 103, 25695-25720, 1998.

Tilmes, S., Lamarque, J.-F., Emmons, L., Conley, A., Schultz, M., Saunois, M., Thouret, V., Thompson, A., Oltmans, S., and Johnson, B.: Ozonesonde climatology between 1995 and 2011: description, evaluation and applications, Atmospheric Chemistry and Physics, 12, 7475-7497, 2012.

Van Malderen, R., Allaart, M. A., De Backer, H., Smit, H. G., and De Muer, D.: On instrumental errors and related correction strategies of ozonesondes: possible effect on calculated ozone trends for the nearby sites Uccle and De Bilt, Atmospheric Measurement Techniques, 9, 3793-3816, 2016.

Wang, G., Kong, Q., Xuan, Y., Wan, X., Chen, H., and Ma, S.: Development and application of ozonesonde system in China, Advances in Earth Science, 18, 471, 2003.

Wang, H. J., Cunnold, D. M., Thomason, L. W., Zawodny, J. M., and Bodeker, G. E.: Assessment of SAGE version 6.1 ozone data quality, Journal of Geophysical Research: Atmospheres, 107, ACH 8-1-ACH 8-18, 2002.

Wild, O., Voulgarakis, A., O'Connor, F., Lamarque, J.-F., Ryan, E. M., and Lee, L.: Global sensitivity analysis of chemistry–climate model budgets of tropospheric ozone and OH: exploring model diversity, Atmospheric Chemistry and Physics, 20, 4047-4058, 2020.

Witte, J. C., Thompson, A. M., Schmidlin, F., Northam, E. T., Wolff, K. R., and Brothers, G. B.: The NASA Wallops Flight Facility digital ozonesonde record: Reprocessing, uncertainties, and dual launches, Journal of Geophysical Research: Atmospheres, 124, 3565-3582, 2019.

Witte, J. C., Thompson, A. M., Smit, H. G., Vömel, H., Posny, F., and Stübi, R.: First reprocessing of Southern Hemisphere ADditional OZonesondes profile records: 3. Uncertainty in ozone profile and total column, Journal of Geophysical Research: Atmospheres, 123, 3243-3268, 2018.

Witte, J. C., Thompson, A. M., Smit, H. G., Fujiwara, M., Posny, F., Coetzee, G. J., Northam, E. T., Johnson, B. J., Sterling, C. W., and Mohamad, M.: First reprocessing of Southern Hemisphere ADditional OZonesondes (SHADOZ) profile records (1998–2015): 1. Methodology and evaluation, Journal of Geophysical Research: Atmospheres, 122, 6611-

https://doi.org/10.5194/egusphere-2024-800
Preprint. Discussion started: 2 April 2024

6636, 2017.

Worden, J., Liu, X., Bowman, K., Chance, K., Beer, R., Eldering, A., Gunson, M., and Worden, H.: Improved tropospheric ozone profile retrievals using OMI and TES radiances, Geophysical Research Letters, 34, 2007.

Xu, W., Xu, X., Lin, M., Lin, W., Tarasick, D., Tang, J., Ma, J., and Zheng, X.: Long-term trends of surface ozone and its influencing factors at the Mt Waliguan GAW station, China–Part 2: The roles of anthropogenic emissions and climate variability, Atmospheric Chemistry and Physics, 18, 773-798, 2018.

Xuan, Y., Ma, S., Chen, H., Wang, G., Kong, Q., Zhao, Q., and Wan, X.: Intercomparisons of GPSO3 and Vaisala ECC ozone sondes, Plateau Meteorology, 23, 394-399, 2004.

Young, P. J., Naik, V., Fiore, A. M., Gaudel, A., Guo, J., Lin, M. Y., Neu, J. L., Parrish, D. D., Rieder, H. E., Schnell, J. L., Tilmes, S., Wild, O., Zhang, L., Ziemke, J., Brandt, J., Delcloo, A., Doherty, R. M., Geels, C., Hegglin, M. I., Hu, L., Im, U., Kumar, R., Luhar, A., Murray, L., Plummer, D., Rodriguez, J., Saiz-Lopez, A., Schultz, M. G., Woodhouse, M. T., and Zeng, G.: Tropospheric Ozone Assessment Report: Assessment of global-scale model performance for global and regional ozone distributions, variability, and trends, Elementa: Science of the Anthropocene, 6, 10.1525/elementa.265, 2018.

Zbinden, R., Thouret, V., Ricaud, P., Carminati, F., Cammas, J.-P., and Nédélec, P.: Climatology of pure tropospheric profiles and column contents of ozone and carbon monoxide using MOZAIC in the mid-northern latitudes (24° N to 50° N) from 1994 to 2009, Atmospheric Chemistry and Physics, 13, 12363-12388, 2013.

Zeng, G., Morgenstern, O., Williams, J. H., O'Connor, F. M., Griffiths, P. T., Keeble, J., Deushi, M., Horowitz, L. W., Naik, V., and Emmons, L. K.: Attribution of stratospheric and tropospheric ozone changes between 1850 and 2014 in CMIP6 models, Journal of Geophysical Research: Atmospheres, 127, e2022JD036452, 2022.

Zeng, Y., Zhang, J., Li, D., Liao, Z., Bian, J., Bai, Z., Shi, H., Xuan, Y., Yao, Z., and Chen, H.: Vertical distribution of tropospheric ozone and its sources of precursors over Beijing: Results from~ 20 years of ozonesonde measurements based on clustering analysis, Atmospheric Research, 284, 106610, 2023.

Zhang, J., Li, D., Bian, J., Xuan, Y., Chen, H., Bai, Z., Wan, X., Zheng, X., Xia, X., and Lü, D.: Long-term ozone variability in the vertical structure and integrated column over the North

https://doi.org/10.5194/egusphere-2024-800
Preprint. Discussion started: 2 April 2024

China Plain: Results based on ozonesonde and Dobson measurements during 2001–2019, Environmental Research Letters, 16, 074053, 2021.

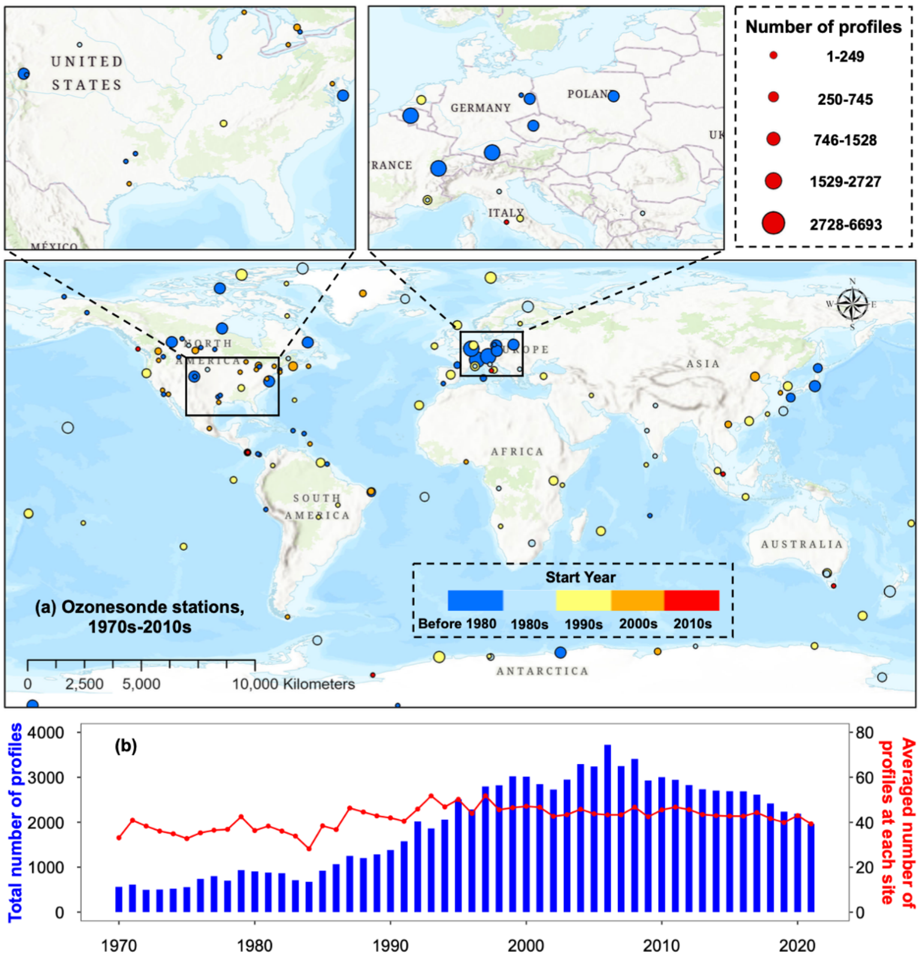

Figure 1. (a) Global distribution of ozonesonde stations used in this study to construct TOST-v2. Station details are provided in Table S1. The size and color of the dots indicate the total number of sounding profiles and the start year of the measurement time series. (b) The total number of profiles per year (left y-axis, blue bars) and the average number of profiles per site and per year

https://doi.org/10.5194/egusphere-2024-800
Preprint. Discussion started: 2 April 2024

(right y-axis, red dots and line) from 1970 to 2021.

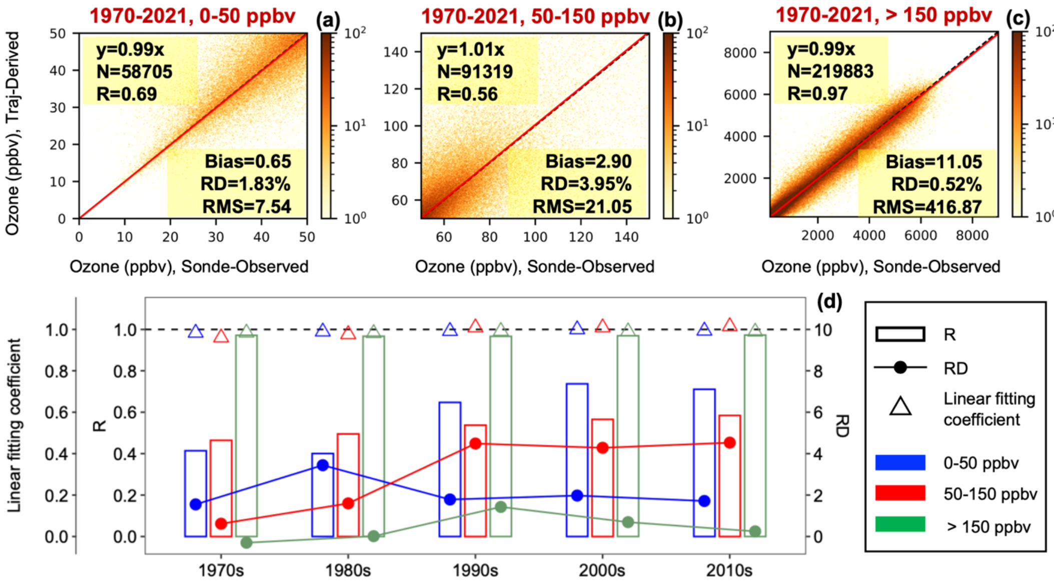

Figure 2. (a-c) Comparison of monthly average tropospheric ozone mixing ratios from ozonesondes (Sonde-Observed) and trajectory-derived TOST data (Traj-Derived) for the entire study period of ozone concentration at 0-50 ppbv, 50-150 ppbv and >150 ppbv. Solid red lines represent the linear fitting line (with the intercept set to 0) and dashed black lines denote the 1:1 axis. N is the total number of data points, R is the correlation coefficient, Bias is the overall average difference in monthly mean values [Traj-Derived ozone - Sonde-Observed ozone, in ppbv], RD is the relative difference in % [100 × (Traj-Derived ozone - Sonde-Observed ozone)/ Sonde-Observed ozone)], and RMS is the root mean square difference in ppbv). Note that Traj-Derived ozone at each station is derived without input from the station itself; that is, Traj-Derived represents an ensemble of 141 separate computations of TOST, each one withholding a single validation station. (d) the R (bars), RD (dots and lines) and linear fitting coefficient (with the intercept set to 0; triangles) between the Traj-Derived ozone and Sonde-Observed ozone by decade. The dashed line denotes where the linear fitting coefficient is 1.

https://doi.org/10.5194/egusphere-2024-800
Preprint. Discussion started: 2 April 2024

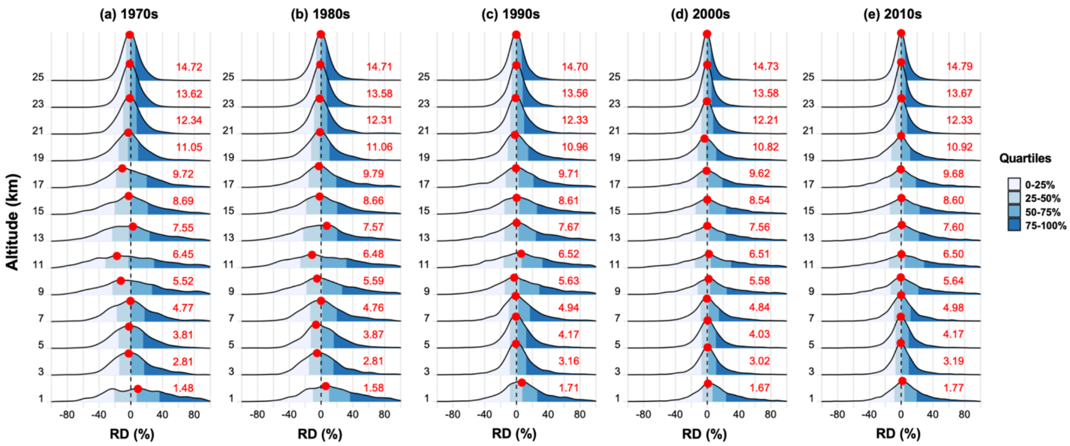

Figure 3. The relative difference (RD) of the monthly ozone mixing ratios between ozonesonde and Traj-Derived data by altitude in the 1970s, 1980s, 1990s, 2000s and 2010s, respectively. The frequency distribution of RD at every other altitudes is shown (y-axis: frequency in %, x-axis: RD in %), with the colors denoting the 4 quartiles of RD. The dashed line indicates zero difference in RD. The red dot and number represent the maximum frequency and the corresponding frequency value in %, respectively.

https://doi.org/10.5194/egusphere-2024-800
Preprint. Discussion started: 2 April 2024

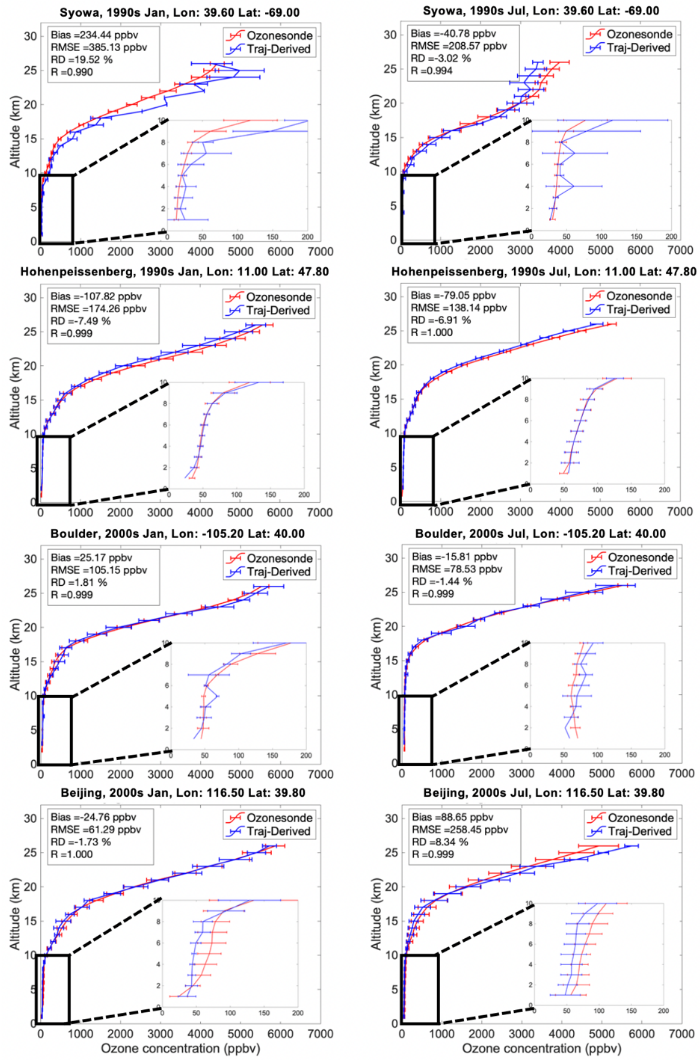

Figure 4. Decadal monthly mean ozone profiles at Syowa and Hohenpeissenberg in January and July 1990s, and at Boulder and Beijing in January and July 2000s. The red line denotes ozonesonde ozone and the blue line denotes trajectory-derived ozone without the input from the station itself. The error bar is ±2 times the standard error of the mean (equivalent to 95 % confidence limits on the averages). To better compare the difference of ozone profiles in the troposphere, a zoom-in window from 0-10 km is provided in each sub-figure.

https://doi.org/10.5194/egusphere-2024-800
Preprint. Discussion started: 2 April 2024

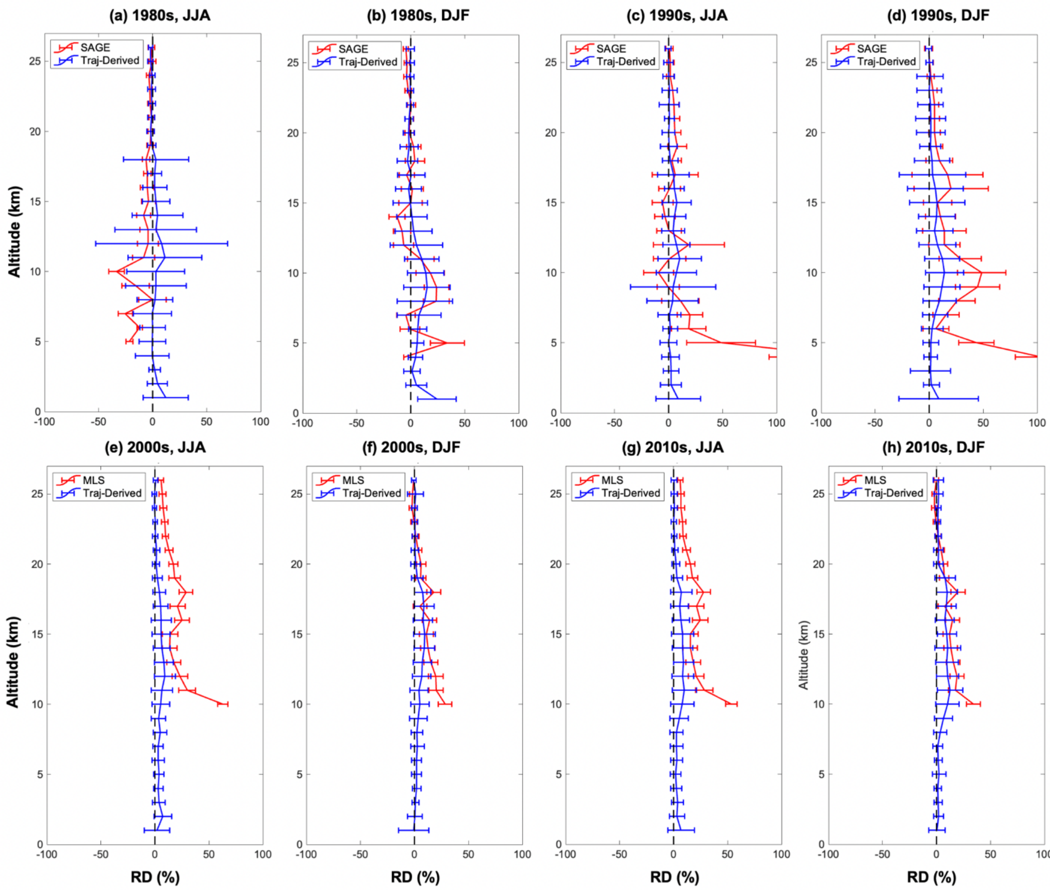

Figure 5. (a-d) Mean relative difference (RD) of the monthly ozone mixing ratios between the Traj-Derived and ozonesonde data (blue line) and between the SAGE and ozonesonde data (red line) in JJA (June-July-August) and DJF (December-January-February), in the 1980s and 1990s. (e-h) Decadal seasonal mean RD between the trajectory-derived and ozonesonde data (blue line) and between the MLS and ozonesonde data (red line) in JJA and DJF, in the 2000s and 2010s. The error bars represent ±1 standard deviation of the seasonal mean RDs at each altitude in each decade.

https://doi.org/10.5194/egusphere-2024-800
Preprint. Discussion started: 2 April 2024

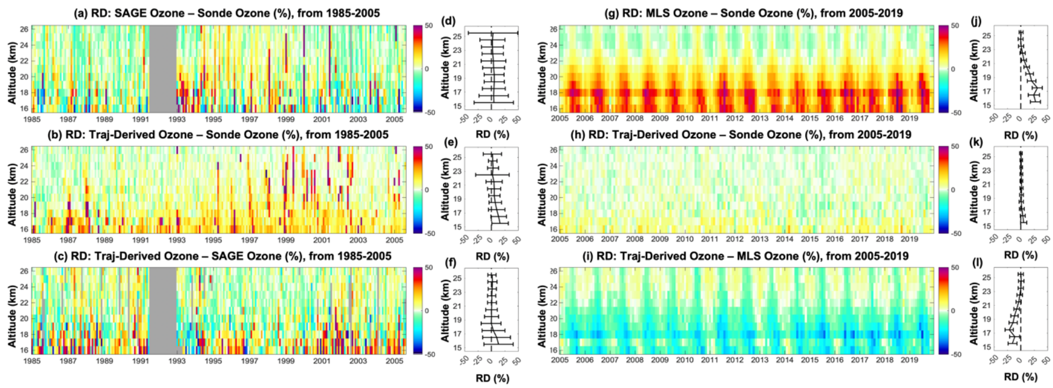

Figure 6. (a). The relative difference (RD) between ozonesonde and SAGE ozone data in each month and at each altitude during 1985-2005 over 16-26 km [RD = 100×(SAGE ozone – ozonesonde ozone)/ozonesonde ozone, in %]. The mean RD over 1985-2005 at each level is shown on the right, where the error bars represent the standard deviation of the monthly RD over 1985-2005. Note that the Pinatubo-affected SAGE profiles are excluded during July 1991- December 1992 (filled with gray color). (b) same as (a), but for the RD between ozonesondes and Traj-derived data, [RD = 100×(Traj-derived ozone – ozonesonde ozone)/ozonesonde ozone, in %]. (c) same as (a), but for the RD between Traj-derived and SAGE ozone data [RD = 100 × (Traj-derived ozone – SAGE ozone)/(0.5 × Traj-derived ozone + 0.5 × SAGE ozone), in %]. (d-f) the averaged RD by altitude corresponding to (a-c). (g-l) same as (a-f), but for the period of 2005-2019 and the satellite measurements are from MLS ozone.

https://doi.org/10.5194/egusphere-2024-800
Preprint. Discussion started: 2 April 2024

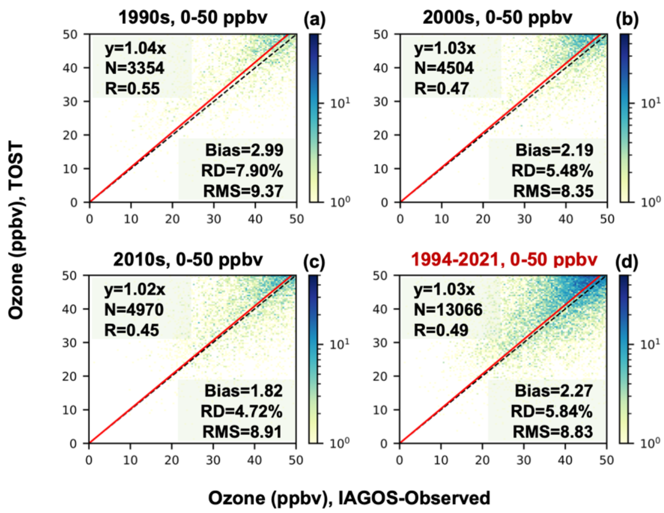

Figure 7. The comparison of monthly ozone mixing ratios between IAGOS-observed (x-axis labeled: IAGOS-Observed) and TOST data (y-axis labelled: TOST) by decade (a-c) and for the entire study period (d) of ozone concentration at 0-50 ppbv. Solid red lines represent the linear fitting line (with the intercept set to 0) and dashed black lines denote the 1:1 axis. N is the total number of data points, R is the correlation coefficient (unitless), Bias is the difference in monthly mean values [TOST ozone - IAGOS ozone, unit: ppbv], RD is the relative difference [100 × (TOST ozone - IAGOS ozone)/(0.5 × TOST ozone + 0.5 × IAGOS ozone)], and RMS the root mean square difference (unit: ppbv).

https://doi.org/10.5194/egusphere-2024-800
Preprint. Discussion started: 2 April 2024

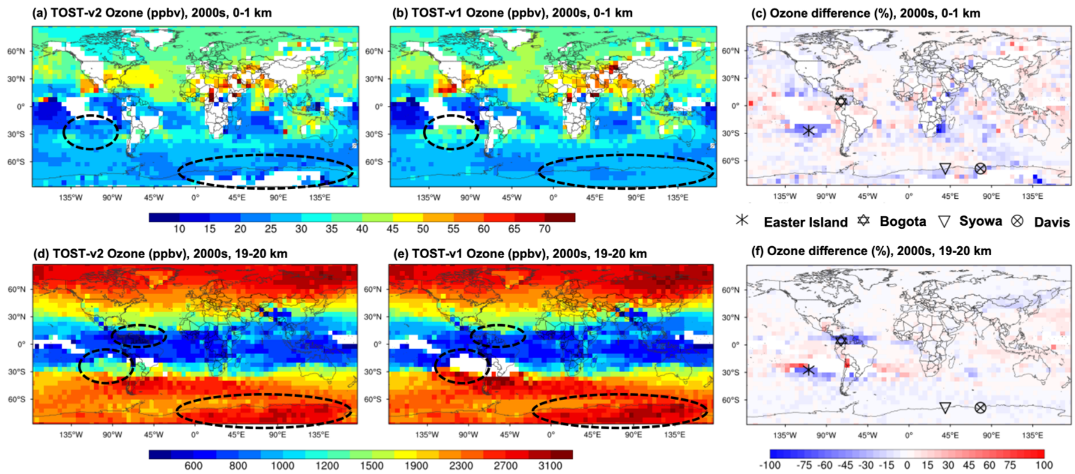

Figure 8. (a, b) The global distributions of ozone in TOST-v2 (a) and TOST-v1 (b) over 0-1 km in the 2000s. (d, e) The same as for (a, b), but over 19-20 km. The dashed circles indicate regions with large differences between the two versions. (c) The global distributions of RD between TOST-v2 and TOST-v1 [RD = 100 × (TOST-v2 – TOST-v1)/(0.5 × TOST-v2 + 0.5 × TOST-v1), in %] over 0-1 km in the 2000s. (f) The same as for (c), but over 19-20 km. The markers indicate the positions of Davis, Easter Island, Bogota and Syowa stations.

https://doi.org/10.5194/egusphere-2024-800
Preprint. Discussion started: 2 April 2024

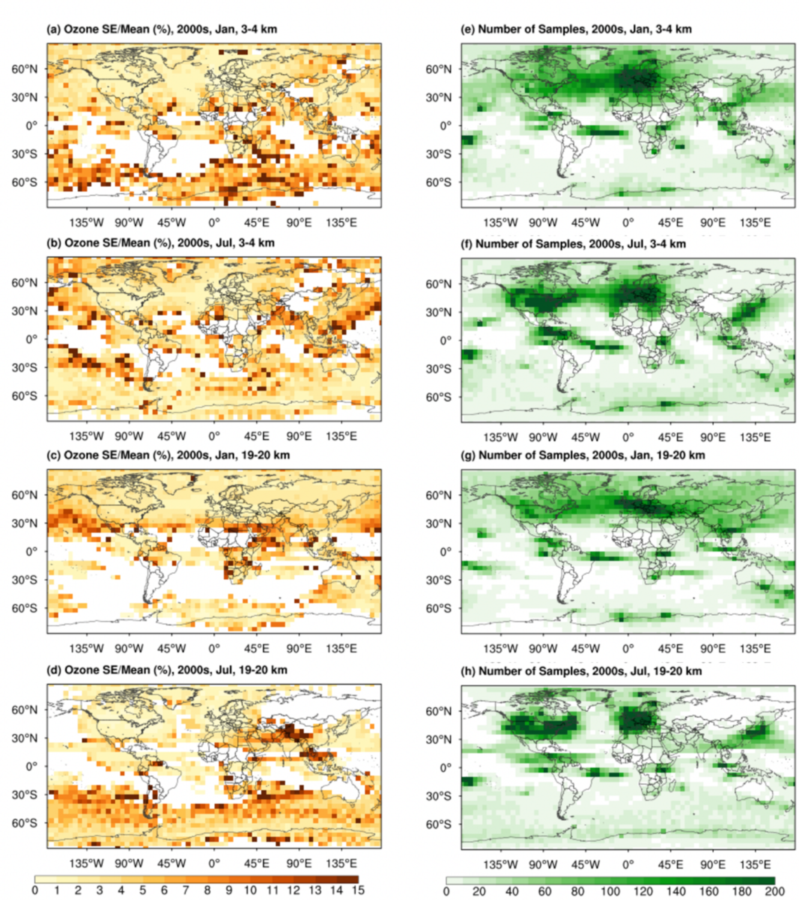

Figure 9. (a-d) Global distribution of the standard error of the mean (left panels, in %) for the decadal monthly mean ozone in January and July 2000s at 3-4 km (a and b) and 19-20 km (c and d). (e-h) the same as (a-d), but for the number of samples in each 5 × 5° bin.

https://doi.org/10.5194/egusphere-2024-800
Preprint. Discussion started: 2 April 2024

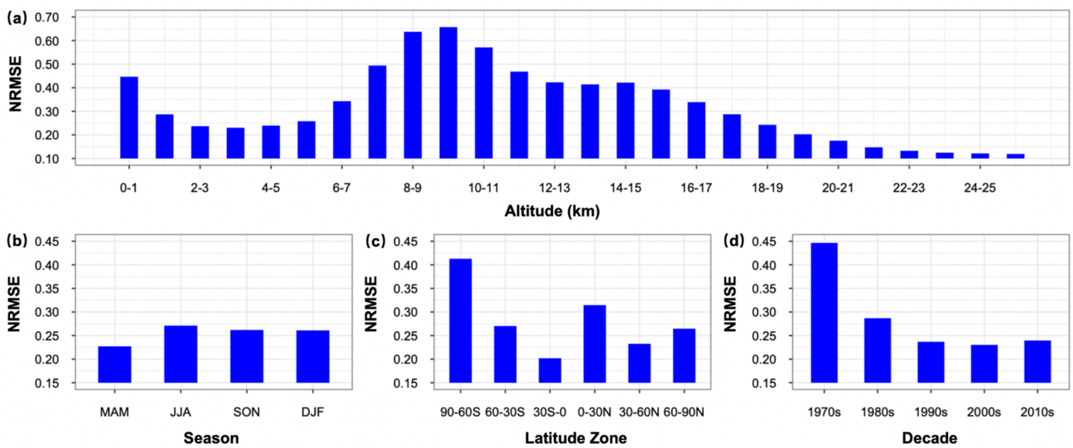

Figure 10. The Normalized Root Mean Squared Error (NRMSE, unitless) of TOST over 1990-2021 by altitude, and the average NRMSE over all altitudes by (a), season (b), latitudinal zone (c), and decade (d). The NRMSE is calculated as the RMS difference of monthly ozone mixing ratio between ozonesondes and Traj-Derived ozone divided by the mean ozone mixing ratio from ozonesondes measurements.

https://doi.org/10.5194/egusphere-2024-800
Preprint. Discussion started: 2 April 2024

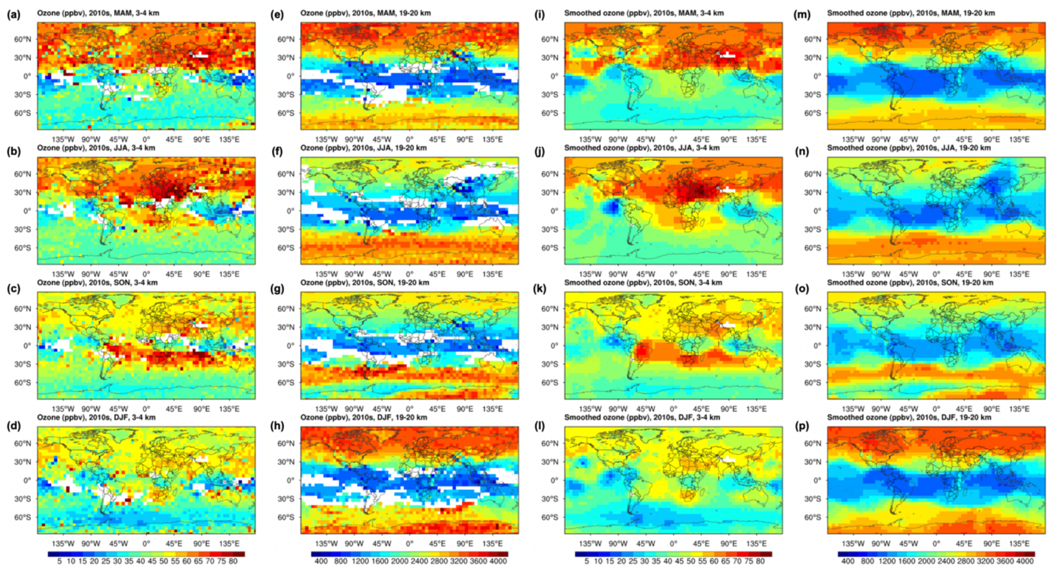

Figure 11. Global distribution of decadal mean TOST ozone at 3-4 km and 19-20 km in MAM (March-April-May), JJA (June-July-August), SON (September-October-November) and DJF (December-January-February) in the 2010s (a-h), and the corresponding smoothed TOST ozone (i-p).

https://doi.org/10.5194/egusphere-2024-800
Preprint. Discussion started: 2 April 2024

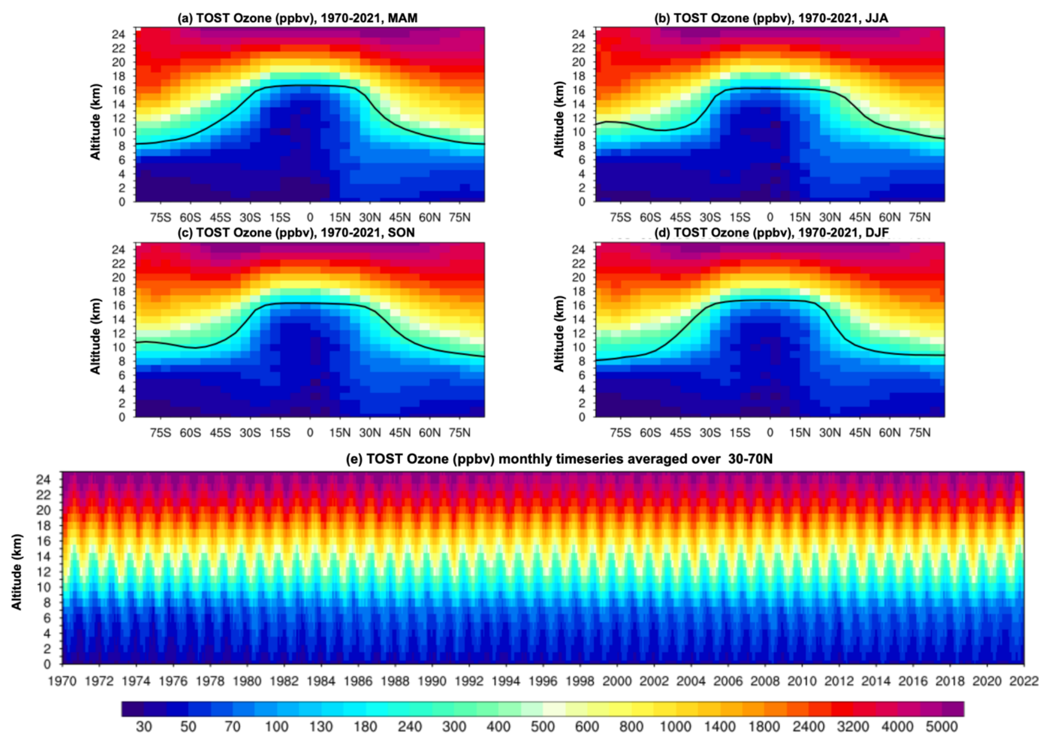

Figure 12. (a-d) The latitude-altitude distribution of TOST ozone averaged over 1970-2021 in each season. The solid black lines represent the mean tropopause height over 1970-2021 in each season. (e) time series of the monthly mean TOST ozone over 30-70°N at each altitude level from 1970 to 2021.

https://doi.org/10.5194/egusphere-2024-800
Preprint. Discussion started: 2 April 2024

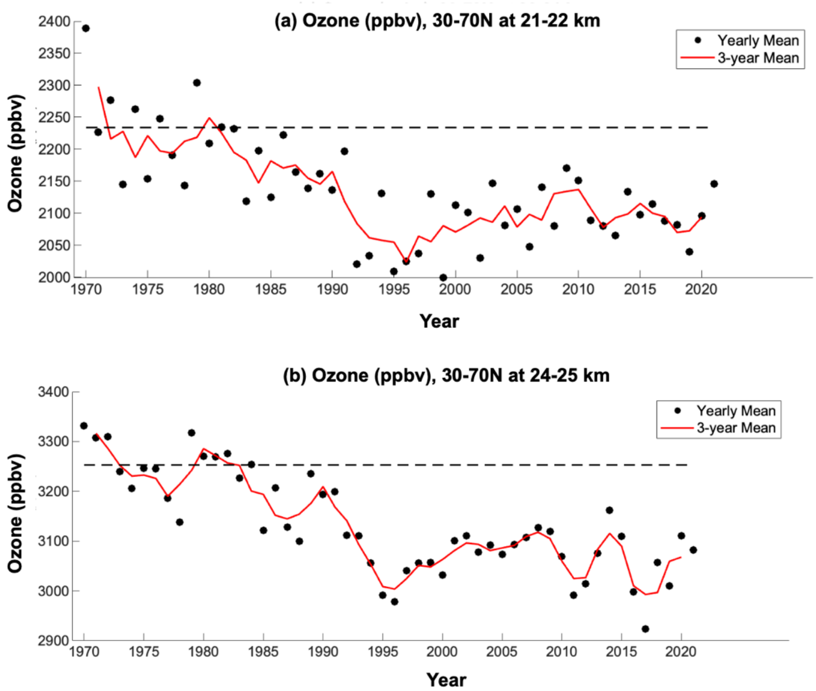

1033

1034 Figure 13. TOST time series of the annual mean ozone mixing ratios averaged over 30-70°N over
1035 21-22 km altitude (a) and 24-25 km altitude (b). The black dots represent the annual mean ozone
1036 concentrations from the area-weighted average of the gridpoints over 30-70°N with ozone data
1037 throughout 1970-2021. The red line is the 3-year running mean. The black dashed line indicates
1038 the average ozone concentrations in the 1970s.